Integrated study of the post-collisional Miocene-Quaternary volcanic forms in the East Carpathians using geological and geophysical constraints

(InstEC - Project code: PN-II-ID-PCE-2012-4-0137)

2014-2nd stage

Budget 2014
In LEI

Salaries	158656,00
Inventory	18775,00
Mobility	54750,00
Overhead (23,16%)	53634,00
Total	285815,00

THE STRUCTURE OF RESEARCH ACTIVITIES

The research was following several objectives/activities in correlation with the research plan:

A. ACTIVITIES RELATED TO BUILDING A GIS DATABASE

(2) 1. BUILDING UP THE GEOLOGICAL AND GEOPHYSICAL GIS COMPATIBLE COMPUTER DATABASE (II)

(2) 1.1. ORGANIZING GEOLOGICAL DATA BASE

In this stage have been corelated to the existing geological map 1:1.000.000 a number of 17 frames (Fig 1), each of them containing ca. 570.000 admissions in attribute type tables of the digital model of the ground that will be used for generation of the final geological and geophysical maps. (Fig. 2).

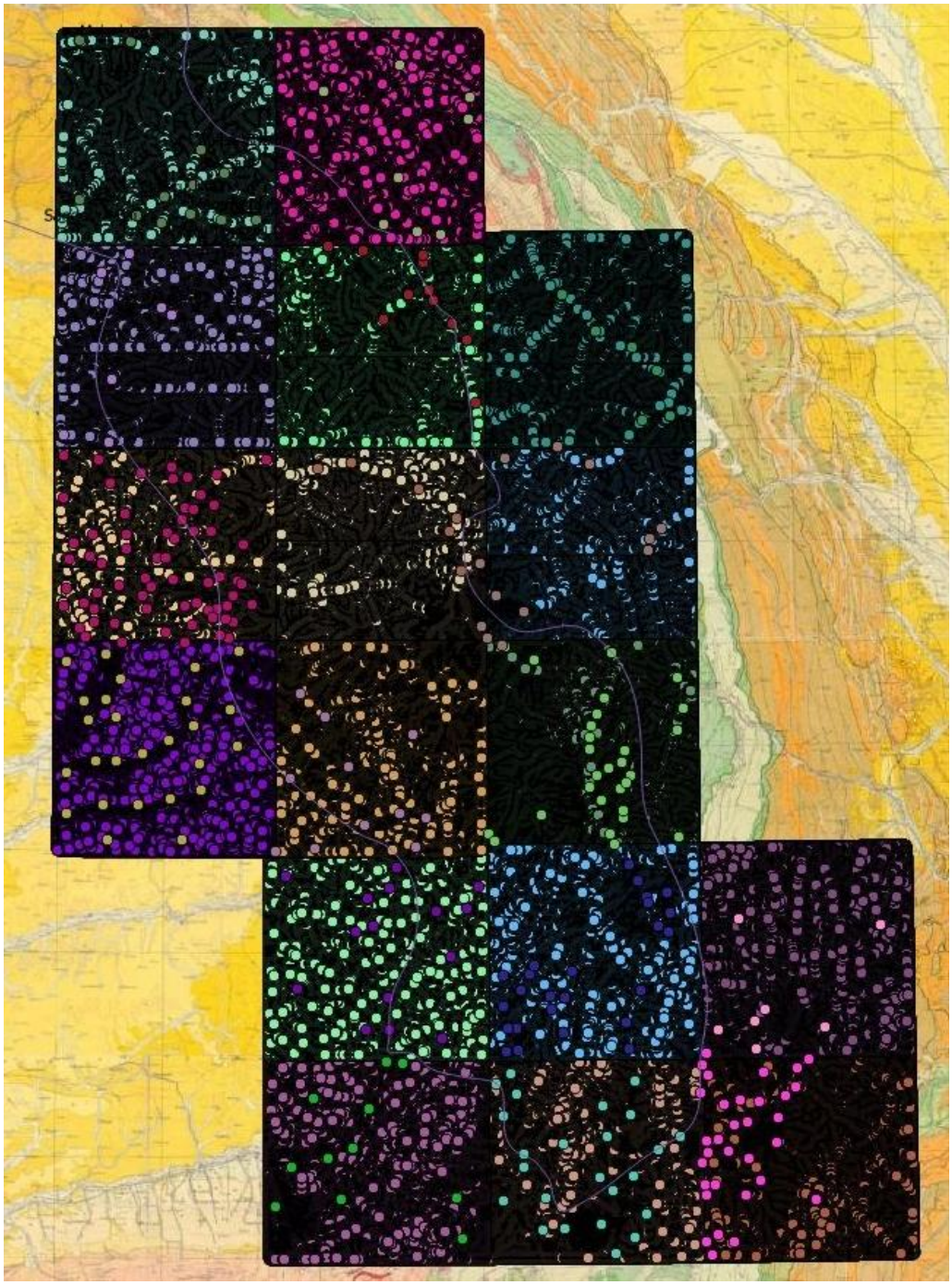

Fig. 1. **Digital model of the ground for the established INSTEC territory supperimpozed to the geological map 1.1000000 (IGR version).**

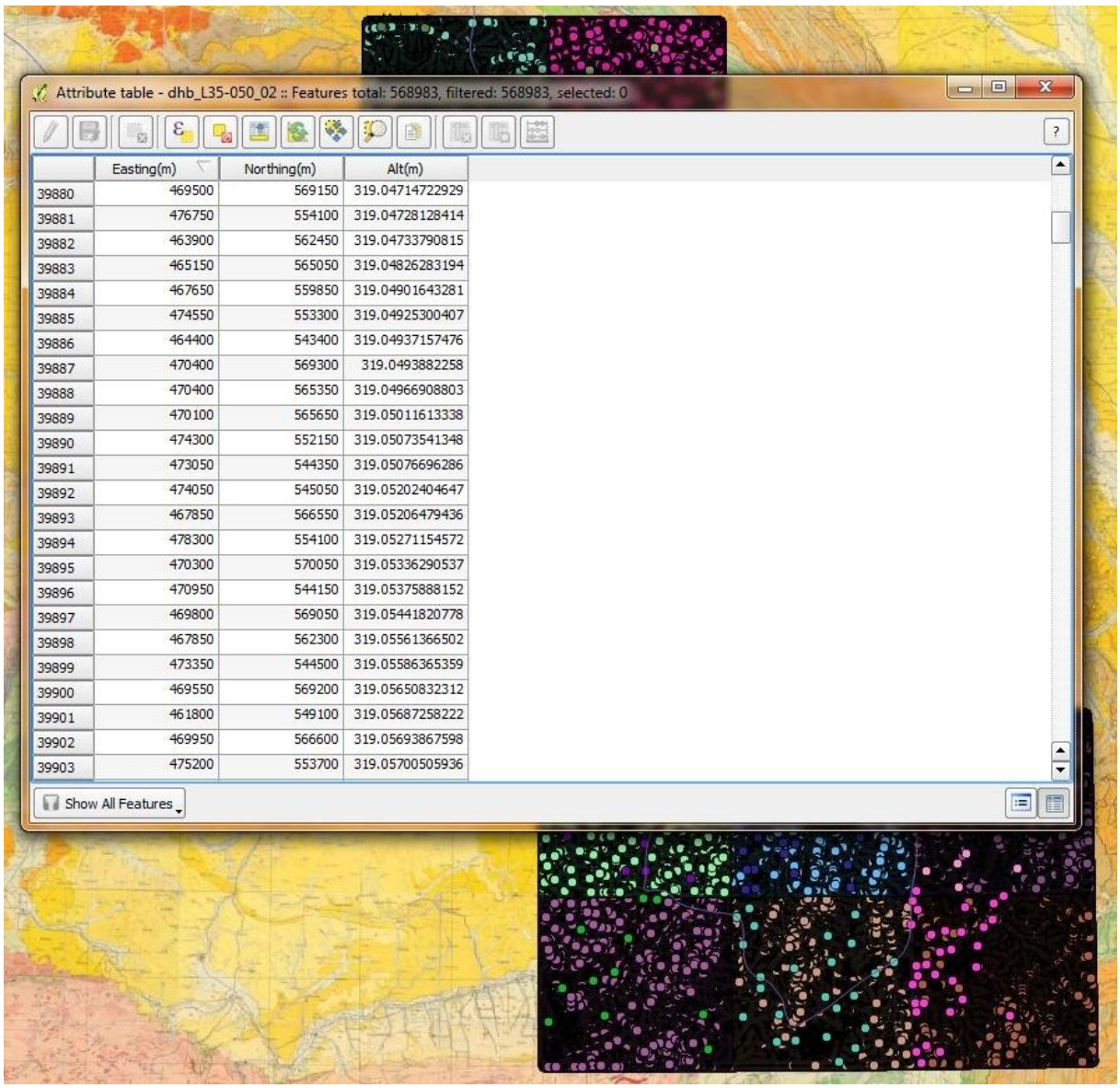

	Easting(m)	Northing(m)	Alt(m)
39880	469500	569150	319.04714722929
39881	476750	554100	319.04728128414
39882	463900	562450	319.04733790815
39883	465150	565050	319.04826283194
39884	467650	559850	319.04901643281
39885	474550	553300	319.04925300407
39886	464400	543400	319.04937157476
39887	470400	569300	319.0493882258
39888	470400	565350	319.04966908803
39889	470100	565650	319.05011613338
39890	474300	552150	319.05073541348
39891	473050	544350	319.05076696286
39892	474050	545050	319.05202404647
39893	467850	566550	319.05206479436
39894	478300	554100	319.05271154572
39895	470300	570050	319.05336290537
39896	470950	544150	319.05375888152
39897	469800	569050	319.05441820778
39898	467850	562300	319.05561366502
39899	473350	544500	319.05586365359
39900	469550	569200	319.05650832312
39901	461800	549100	319.05687258222
39902	469950	566600	319.05693867598
39903	475200	553700	319.05700505936

Fig. 2 Example of attribute type tables used for the digital model supperimpozed to the geological map 1.1000000 (IGR version)

As well, in this stage was evaluated the distribution along the Călimani-Gurghiu-Harghita volcanic chain, of a series of already published maps at the scale 1:50000, published by Geological Institute of Romania (Fig. 3). In the next stage the maps will be correlated and simplified with a new legend in a modern style with complex attribute tables.

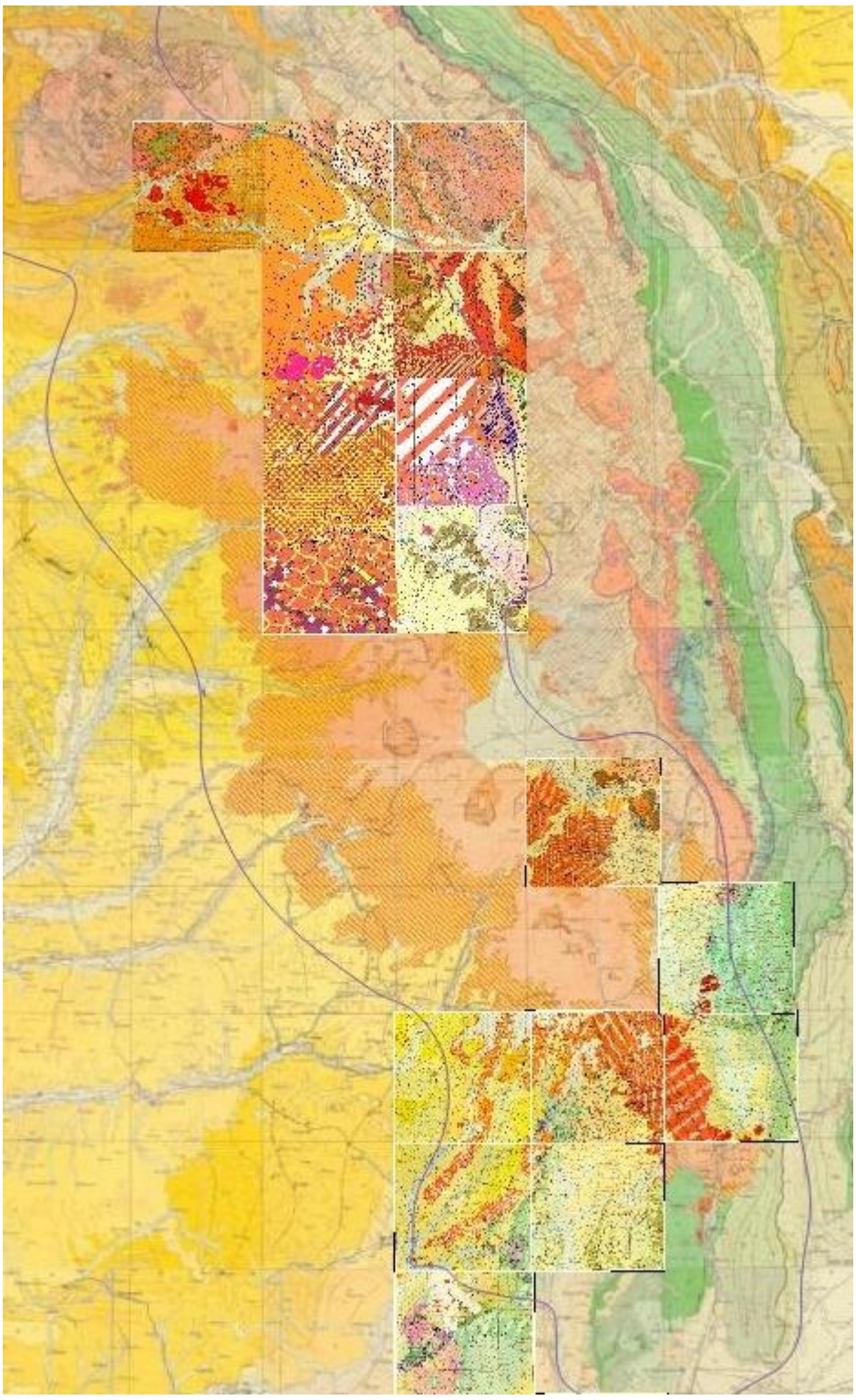

Fig. 3. **Supperimpozed 1:50000 geological maps on the geological map 1.1000000 (all IGR version)**

(2) 1.2. THE TRANSFER OF THE GRAVITY INFORMATION ON ELECTRONIC SUPPORT AND DATABASE VALIDATION

A thorough review of the literature has revealed several papers useful to extract gravity information related to our project: Mocanu şi Radulescu (1994), Ioane si Radu (1995), Atanasiu et al. (1996), Hackney et al. (2002), Ioane si Atanasiu (1998), Ioane et al. (2005) and Ioane si Ion (2005).

The most comprehensive of them seems to be Mocanu si Radulescu (1994) offering a synoptic image of the Bouguer anomaly on the whole territory of Romania.

The map published by the above-mentioned authors has been scanned, and digitised by employing the commercial application DIDGER (©Golden Software).

Data has been referred to the stereographic projection system STEREO 1970, and restitution of the gravity field has been provided for the study area by using the GIS compatible application SURFER (©Golden Software).

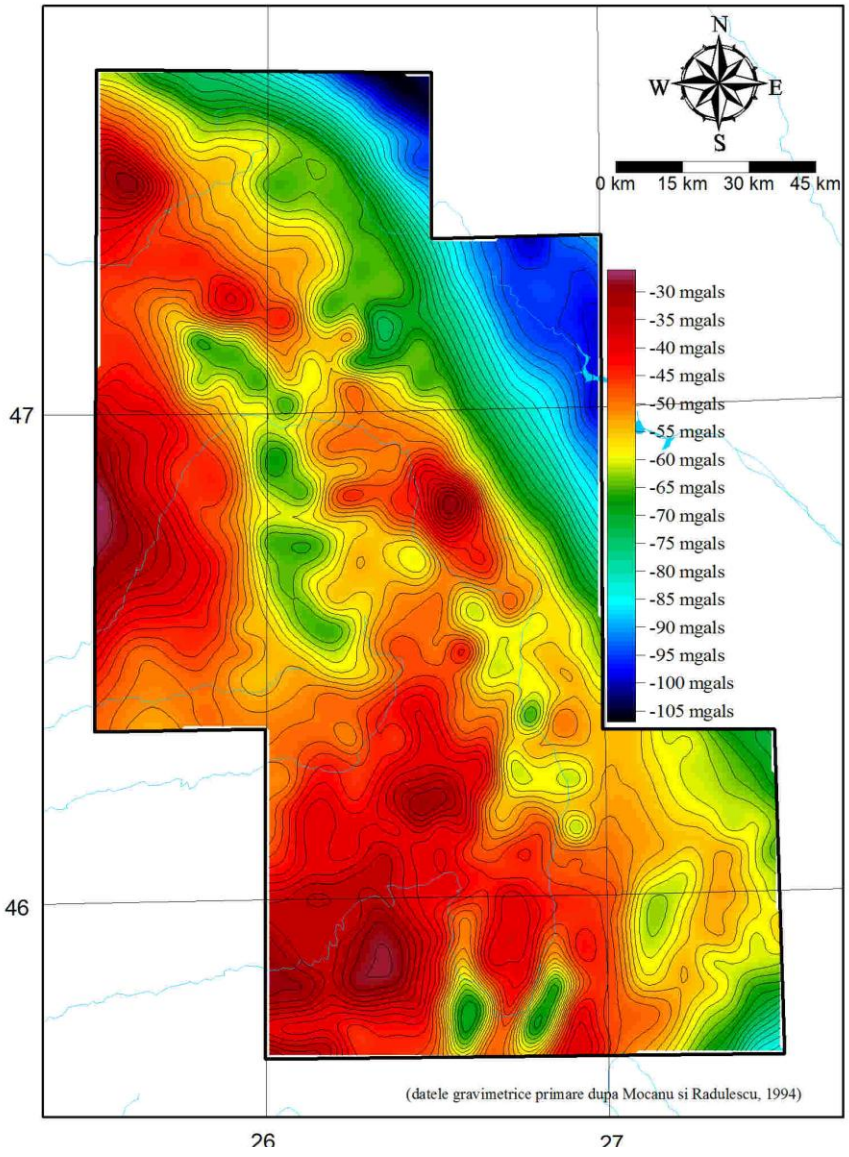

Fig.4 - BOUGUER ANOMALY TREND WITHIN STUDY AREA

(2) 1.3. THE TRANSFER OF THE GROUND GEOMAGNETIC INFORMATION ON ELECTRONIC SUPPORT AND DATABASE VALIDATION

The review of the geophysical literature has pointed out several works dealing with the results of geomagnetic surveys within the study area.
The most comprehensive source is represented by the National Ground Vertical Geomagnetic Map of Romania (Airinei et al, 1983; 1984), providing a consistent image of the vertical component of the geomagnetic field over the whole territory of our country.

The published maps have been scanned and digitised, and information has been organised in the stereographic projection system STEREO 1970 by the help of the computer application DIDGER (©Golden Software).
The restitution of the variation of the vertical component of the geomagnetic field within the study area has been performed by employing the commercial application SURFER (©Golden Software)

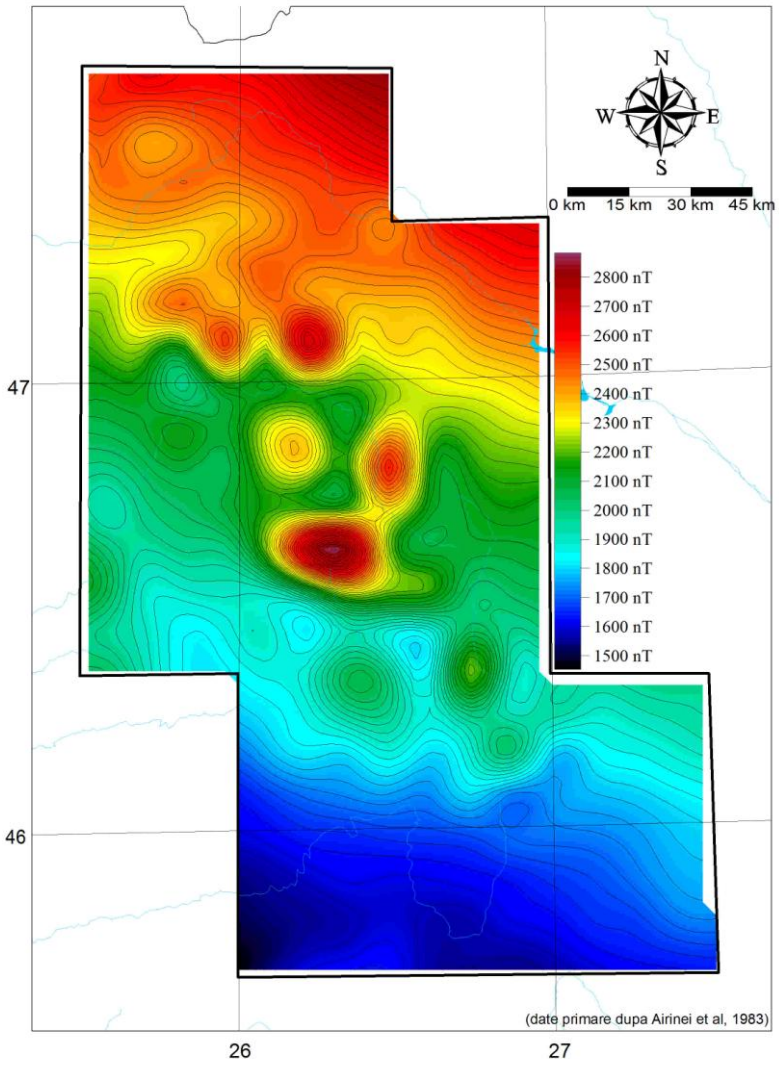

Fig. 5 - **REGIONAL TREND OF THE VERTICAL COMPONENT OF THE GEOMAGNETIC FIELD WITHIN THE STUDY AREA**

(2) 1.4. THE TRANSFER OF THE AEROMAGNETIC INFORMATION ON ELECTRONIC SUPPORT AND DATABASE VALIDATION

The model of the total intensity scalar of the geomagnetic field within the project area has been constructed mainly based on the data provided by World Digital Magnetic Anomaly Map (WDMAM) project as achieved by an international team (e.g. Korhonen et al, 2007).
The project integrates airborne geomagnetic data provided by the participant countries with satellite data and ocean bottom information into a consistent image for the altitude of 5000 meters above the WGS 1984 ellipsoid.

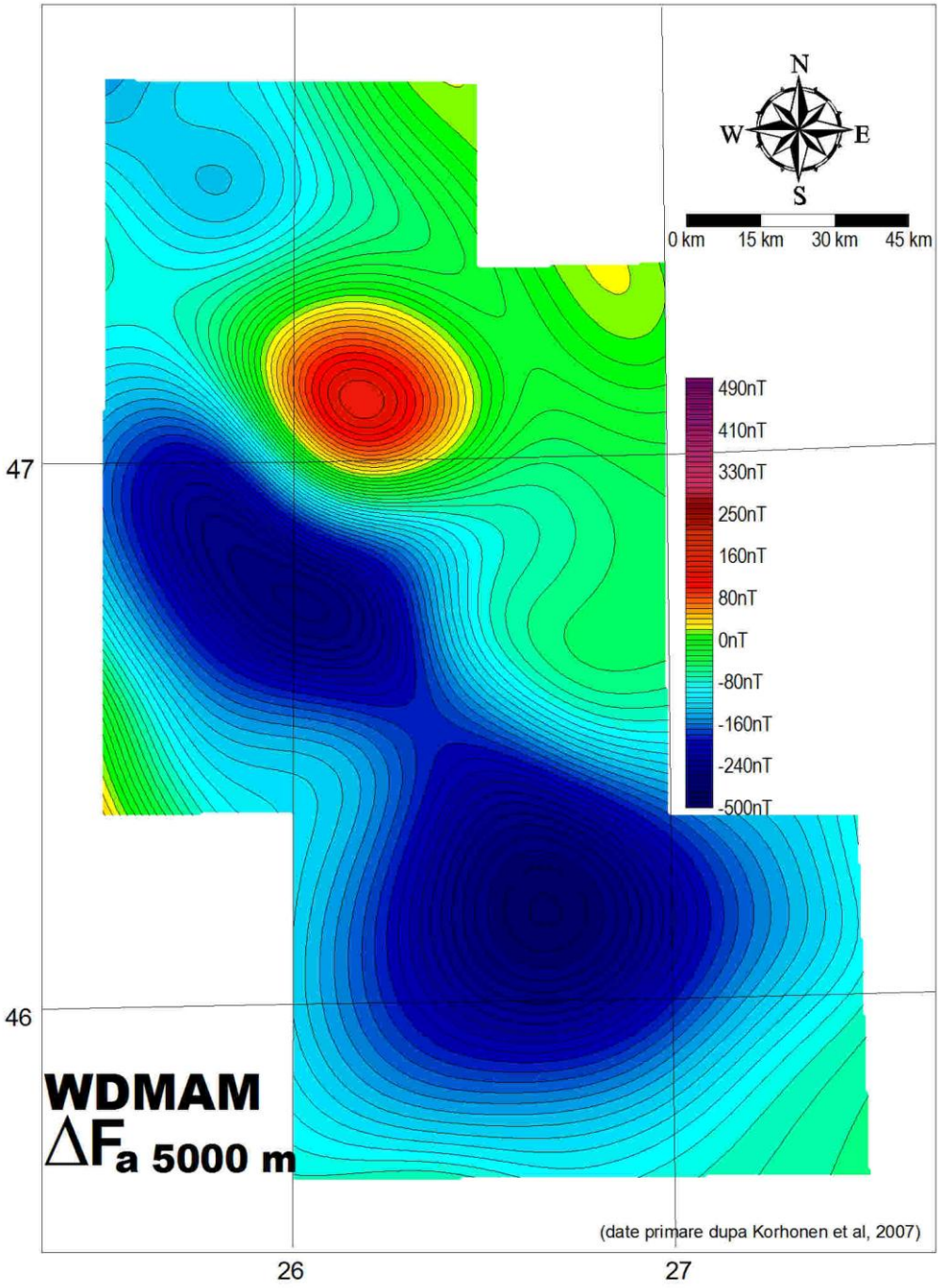

Fig. 6 - TOTAL INTENSITY SCALAR GEOMAGNETIC ANOMALY AT THE ALTITUDE OF 5000 METERS

Following the Romania's decision to participate in WDMAM project a set of aeromagnetic data has been released. The new dataset consisted of a 10 km x 10 km grid of total intensity scalar geomagnetic anomaly, derived from the older regional airborne geomagnetic surveys of the Romanian territory, upward continued at the altitude of 5000 meters (Besutiu et al., 2012).

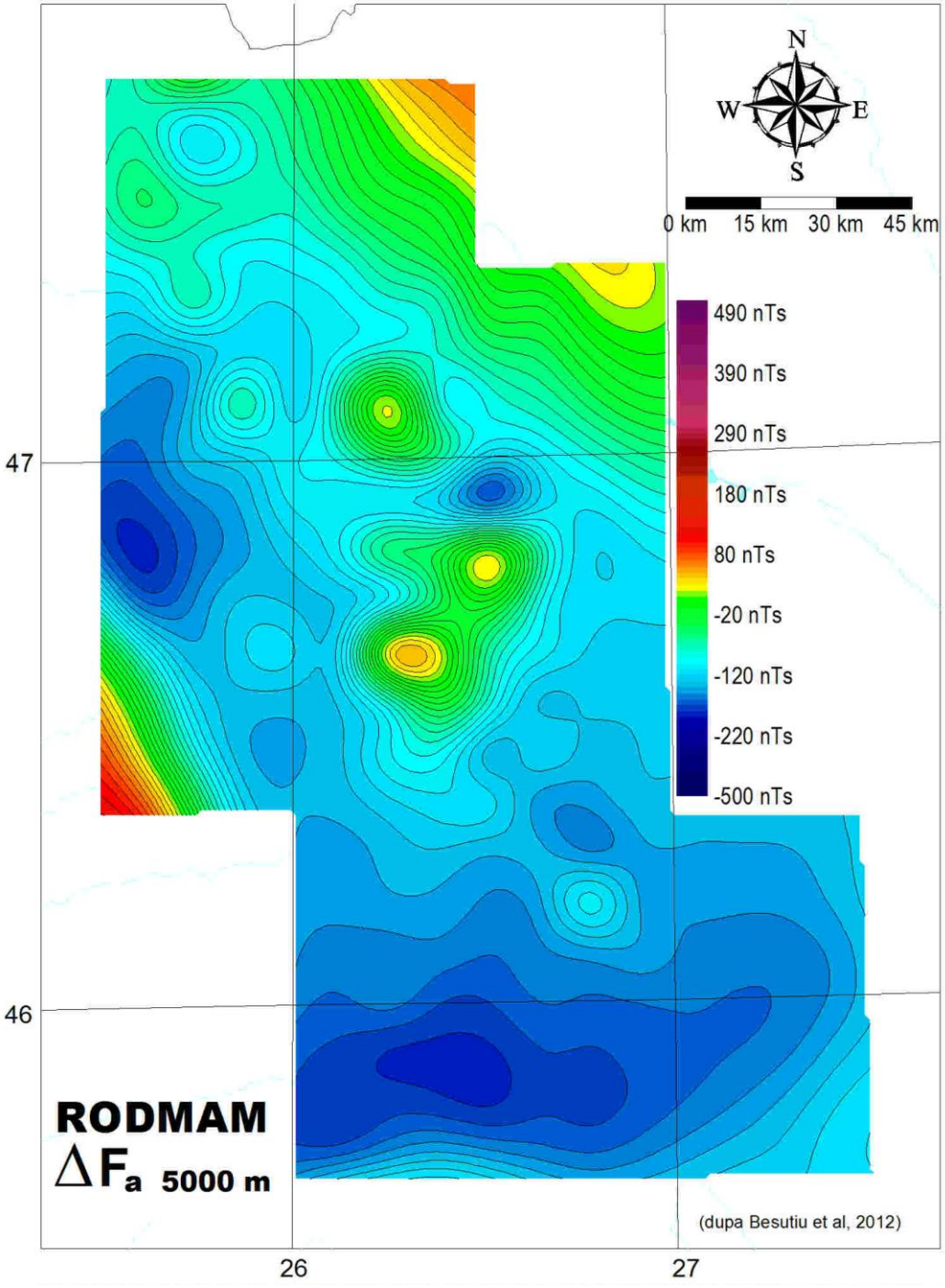

Fig. 7 - TOTAL INTENSITY SCALAR GEOMAGNETIC ANOMALY MODEL BASED ON THE WDMAM - ROMANIAN CONTRIBUTION

(2) 1.5. THE TRANSFER OF ADDITIONAL INFORMATION ON ELECTRONIC SUPPORT AND DATABASE VALIDATION

Among the various geophysical surveys previously conducted in the study area mentions should be made to the EM research performed by Dr. Dumitru Stanica and his co-authors.
The following figure some tentative models for the deep structure of East Carpathians along two lines of magneto-telluric soundings (MTS) as inferred from the interpretation of the MTS data (according to Stanica et al., 1986)

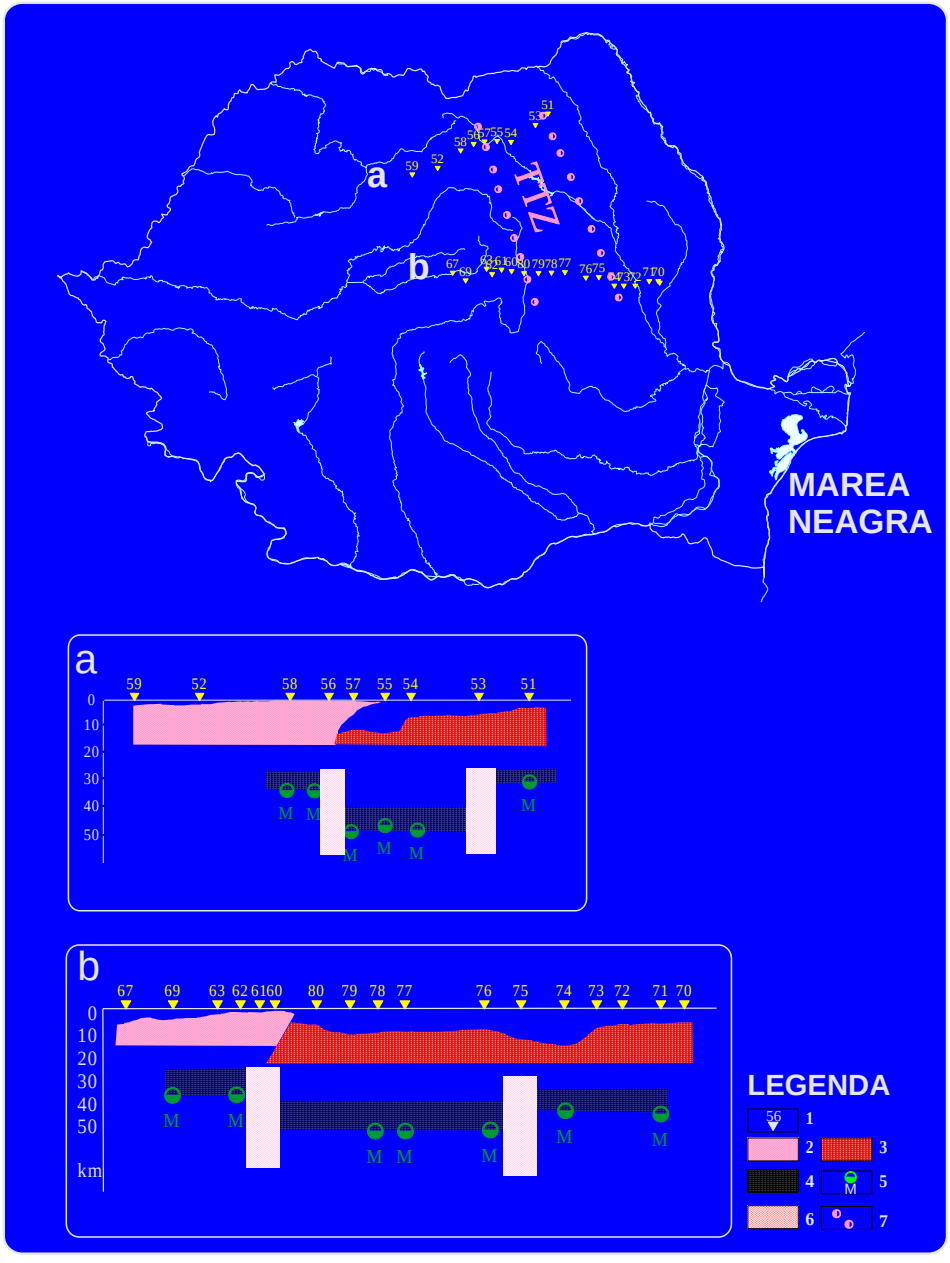

FIG. 8 - DEEP STRUCTURE OF EAST CARPATHIANS AS INFERRED FROM MTS DATA INTERPRETATION (raw MTS data according to Stanica et al, 1986)
1, magnetotelluric sounding location; 2, crystalline basement; 3, upper crust; 4, lower crust; 5, trans-crustal discontinuities; 6, Moho; 7, the assumed track of the Tornquist-Teysseire Zone (TTZ)

(2) 1.6. THE TRANSFER OF ROCK PHYSICS INFORMATION ON ELECTRONIC SUPPORT AND DATABASE VALIDATION

The database concerning the magnetic properties of the main geological formation cropping out in the study area has been constructed mainly based on the inspection of the geophysical literature on the study area.

The next figure shows the location of the outcrops sampled for rock-magnetism studies in Harghita Mts., already reported in 2013 for that have been done additional studies in 2014.

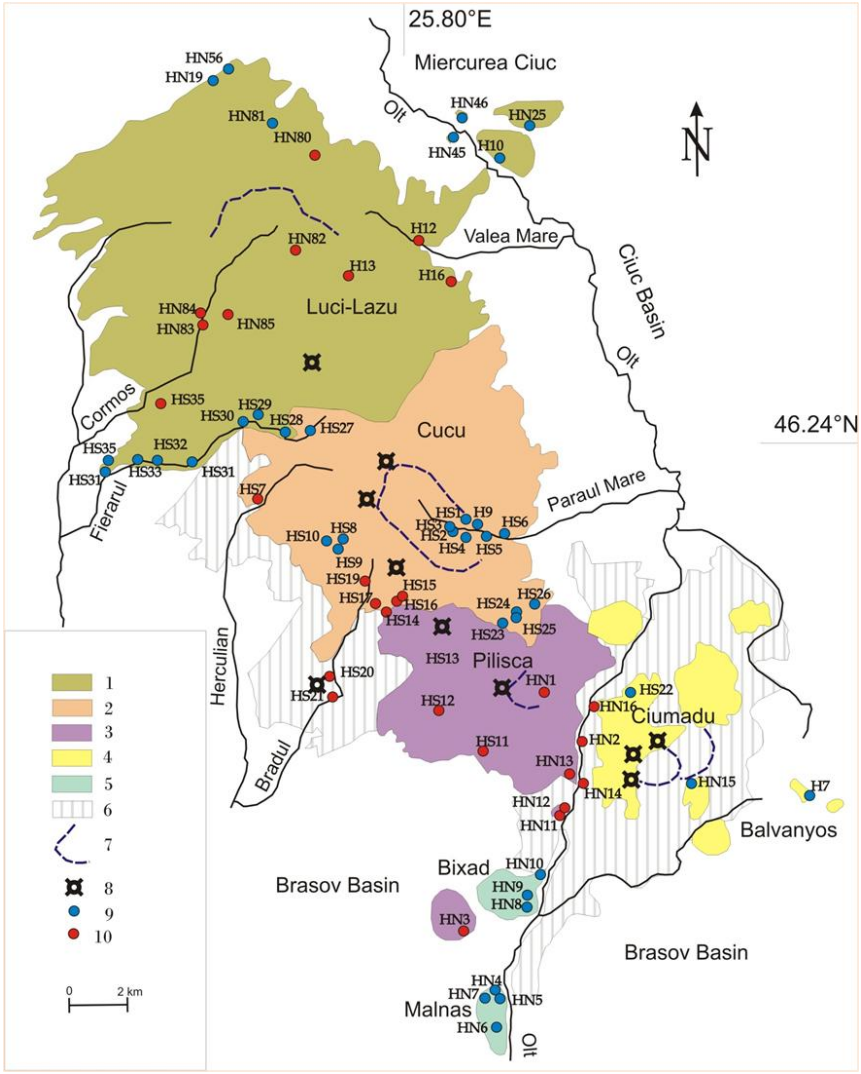

Fig. 9. Location of the sampling points within South Harghita Mts. The geological background is modified after S*eghedi et al., 1987*.

1. Volcanic structures Luci-Lazu şi Şumuleu-Ciuc (4.3 (5.1?)– 3.6 Ma);
2. Volcanic structure Cucu (2.8–2.2 Ma);
3. Volcanic structure Pilişca (2.5–1.5 Ma);
4. Volcanic structure Ciomadul (0.6–0.2 Ma) and the extrusive dom Balvanyos (0.9–1.0 Ma);
5. Intrusive domes Malnaş şi Bixad (2.2–1.4 Ma);
6. Volcanoclastic rocks;
7. Crater;

8. Eruption centre;
9. Sampling point with positive geomagnetic inclination;
10. Sampling point with negative geomagnetic inclination;

(2) 1.7. THE TRANSFER OF DRILLING INFORMATION ON ELECTRONIC SUPPORT AND DATABASE VALIDATION

(2) 1.7.1. Geophysical data

Following the refuse of the National Agency for Mineral Resources to allow the access of the researchers working in the INSTEC project to the information previously obtained in the study area, the amount of data related to drillings performed in the region has been dramatically limited to the few publications revealing data of such a nature.

The thorough review of the literature in the related field revealed some information that might be grouped into two categories:

- stress data, as a result of the investigations of the borehole deformation under the action of the tectonic stress (e.g. Muller, 1993; Zugravescu et al, 2005; Negoita et al, 2007; Zugravescu si Negoita, 2010);

- geothermal data (e.g. Demetrescu et al, 2001; Demetrescu et al, 2005; Veliciu, 1998).

The next figure presents the location of the wells investigated through the "borehole break-out" methodology for stress determinations.

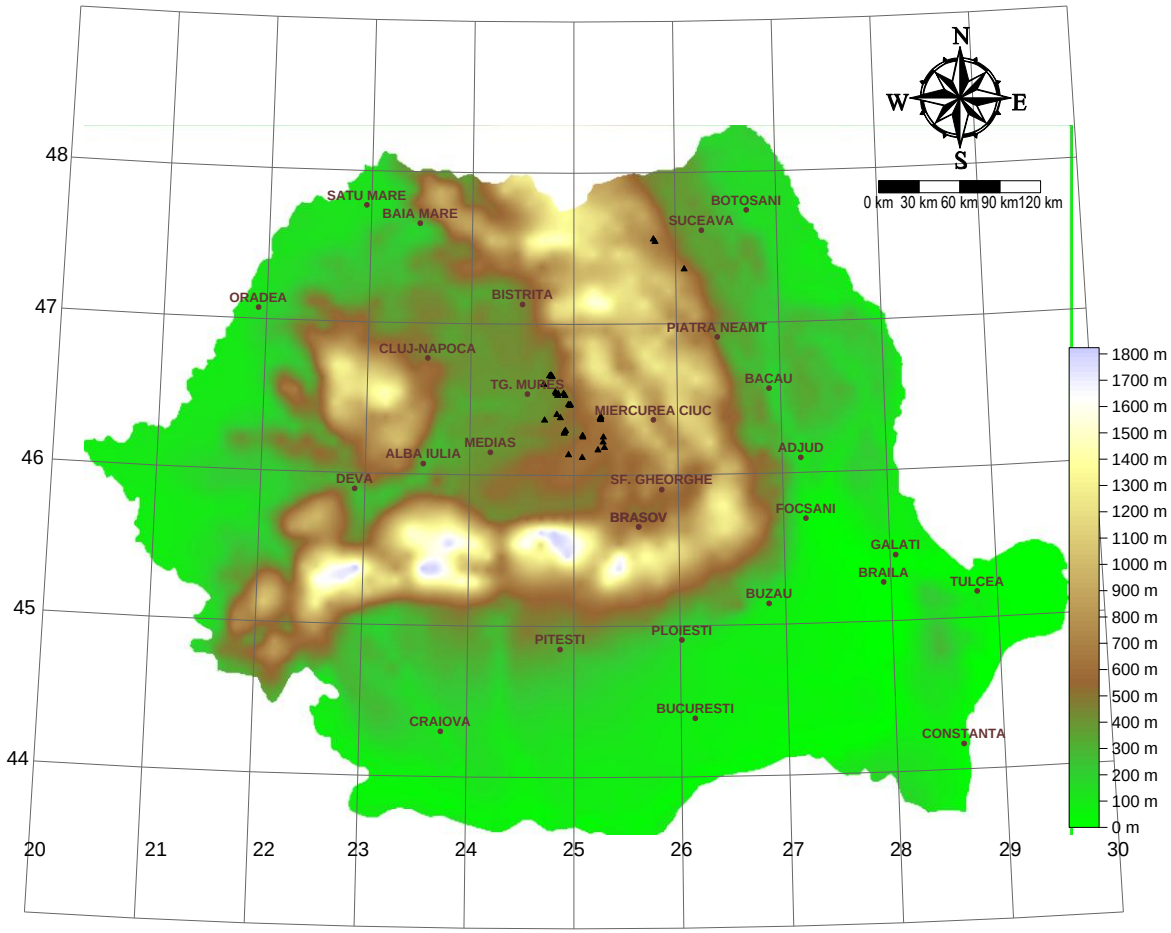

FIG. 10 - LOCATION OF WELLS IN THE STUDY AREA AND NEIGHBOURING REGION WHERE TECTONIC STRESS HAS BEEN DETERMINED

Geothermal investigations targeted the following parameters:

- in-depth temperature evolution

- vertical geo-thermal gradient

- heat-flow estimates

Location of the investigated wells is shown in the next figure:

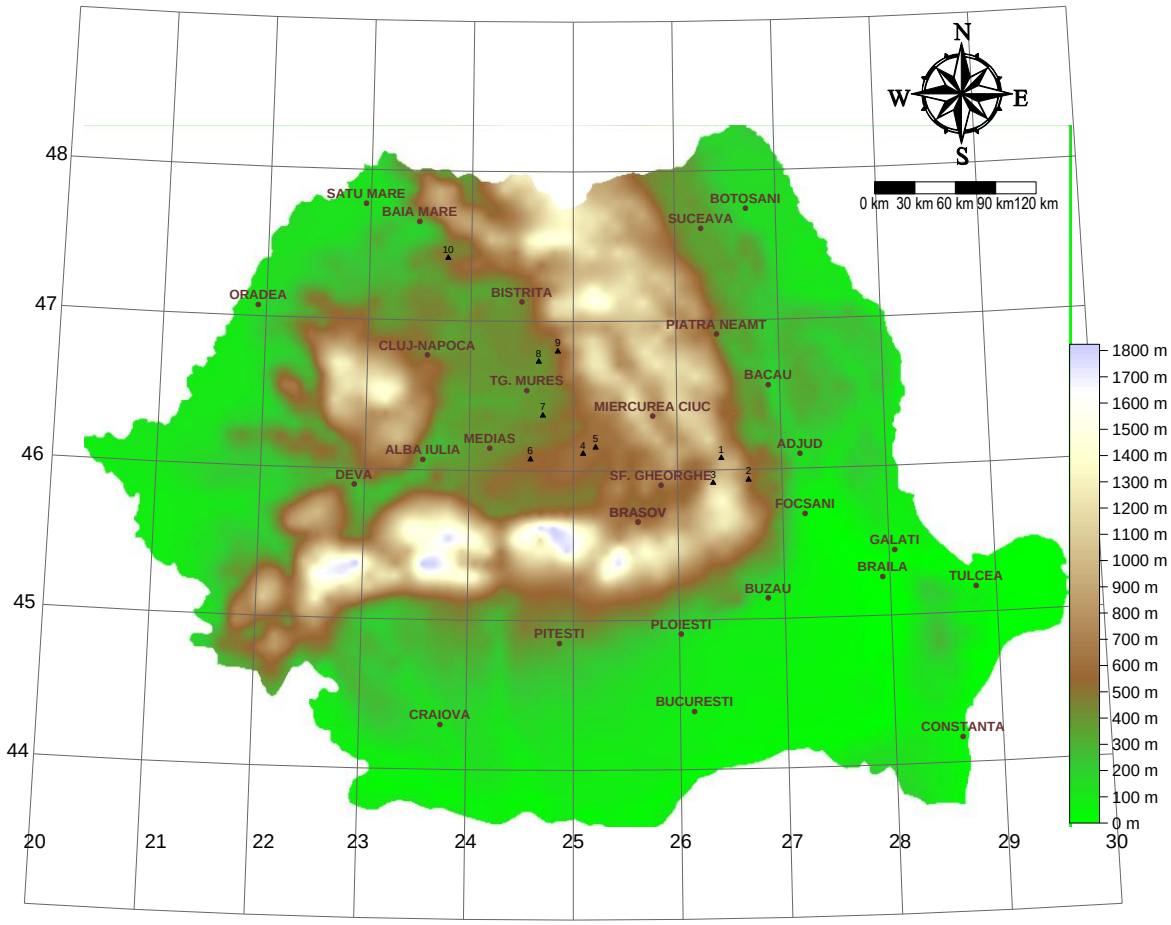

FIG 11 - LOCATION OF THE WELLS IN THE STUDY AREA AND NEIGHBORING REGION WHERE GEOTHERMAL PARAMETERS DETERMINATIONS HAVE BEEN CONDUCTED

(2) 1.7.2. Geological data extraction

Drill-hole Izvorul Alb

In December 2013, a water-based fluid drilling was performed in the Izvorul Alb area, near Dorna Cândrenilor, over a depth of 96 m. The Groundwater Engineering Research Center has kindly provided us with the data resulted from geophysical logging performed in the drill-hole. The standard logging contains information derived from natural gamma radiation, spontaneous potential, 16’ resistivity, 64’ resistivity, temperature and resistance measurements. The geophysical data were interpreted and the lithological model from figure 13 was derived.

Figure 12 – **Location of Izvorul Alb drill-hole**

The drilling pierced pre-volcanic sedimentary formation, of Lutetian age, Eocen epoch, consisted of alternating sandstones, shales and marls. The behavior of the spontaneous potential curve indicates the fact that all sandstones and clayey sandstones hold groundwater, and that the porous formations between 84 m and 96 m depth seem to host mineralized, possibly carbonated waters (lower resistivity, the inflexions of the spontaneous potential curve are accentuated). Carbonation and water mineralization are processes characteristic of volcanic areas, and sometimes associated to post-volcanic activity. The data will be used in further geological and geophysical interpretations.

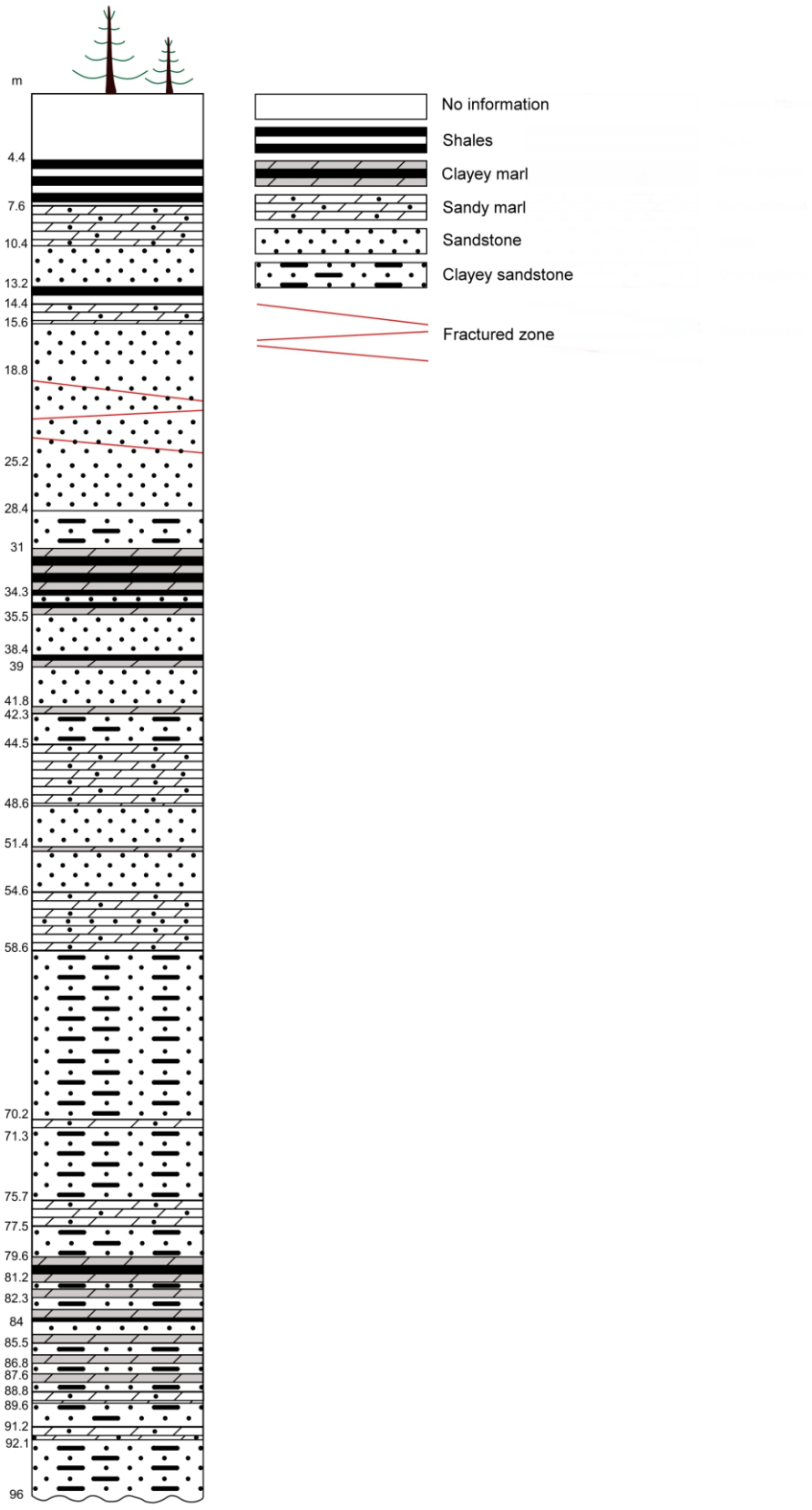

Figure 13 – **The lithologic interpretation of geophysical data from Izvorul Alb drilling**

(2) 1.8. UPDATING THEMATIC DATABASES

(2) 1.8.1. UPDATING THEMATIC DATABASES WITH THE RESULTS OF GEOLOGICAL SURVEYS PERFORMED DURING THE SECOND STAGE

The geological research has followed:

- Regional field investigations within INSTEC-NORD perimeter and south Gurghiu area, where ca. 200 rock sampling and complex geological and tectonic observations have been performed.
- Detailed field geological investigation within Ciomadul and Persani areas, where new geological maps have been realized. The new achievements will be published in ISI journals.
- Laboratory investigation for petrographical observations of the selected collected samples. Initiation the geochemical data base. Initiation the evaluation of the existing K/Ar data.

(2) 1.8.2. UPDATING THEMATIC DATABASES WITH THE RESULTS OF GEOPHYSICAL SURVEYS AND ROCK-PHYSICS PROPERTIES DETERMINATIONS PERFORMED DURING THE SECOND STAGE

During the second stage of the project, geophysical research has developed into two main directions:

- regional investigations within INSTEC-SUD perimeter;
- detailed investigations within CIOMADUL and PERSANI sub-perimeters

As a consequence of the activities performed in the above-mentioned specific areas of the project, the results may be summarized as follows:

TOPOGRAPHIC DATA
- finalization of the digital terrain model for the whole INSTEC area
- outline of the working areas corresponding to various stages of the project accomplishment

GRAVITY DATA
- regional-scale gravity observations within the INSTEC-SUD area
- local gravity survey within CIOMADUL sub-perimeter
- local gravity survey within PERSANI sub-perimeter

GEOMAGNETIC DATA
- field geomagnetic observations (total intensity scalar of the geomagnetic field) within INSTEC-SUD perimeter
- field geomagnetic observations (total intensity scalar of the geomagnetic field) within CIOMADUL sub-perimeter;
- field geomagnetic observations (total intensity scalar of the geomagnetic field) within PERSANI sub-perimeter

ROCK PHYSICS DATA
- density determinations on previously collected rock samples
- density determinations on rock samples collected during 2014 field campaigns

B. ACTIVITIES RELATED TO DATA SYNTESIS

(2) 2. ANALYSIS AND CRITICAL DISCUSSION OF THE CURRENT MODELS ASSOCIATED TO GEODYNAMIC EVOLUTION OF THE EAST CARPATHIANS IN CONNEXION WITH MIOCENE-QUATERNARY MAGMATIC ACTIVITY (II).

(2) 2.1. GRAVITY ECHOES OF THE CURRENT GEOLOGICAL CONCEPT

In order to analyse the echoes of the current geological models of the study area within gravity data, a comparative view between the geological concept and various models of the Bouguer anomaly and its derivatives has been performed.

In the followings, the above-mentioned analysis is distinctly presented for the southern part of the INSTEC perimeter, the so-called INSTEC-SUD area, with some detailed images provided for CIOMADUL and PERSANI sub-perimeters.

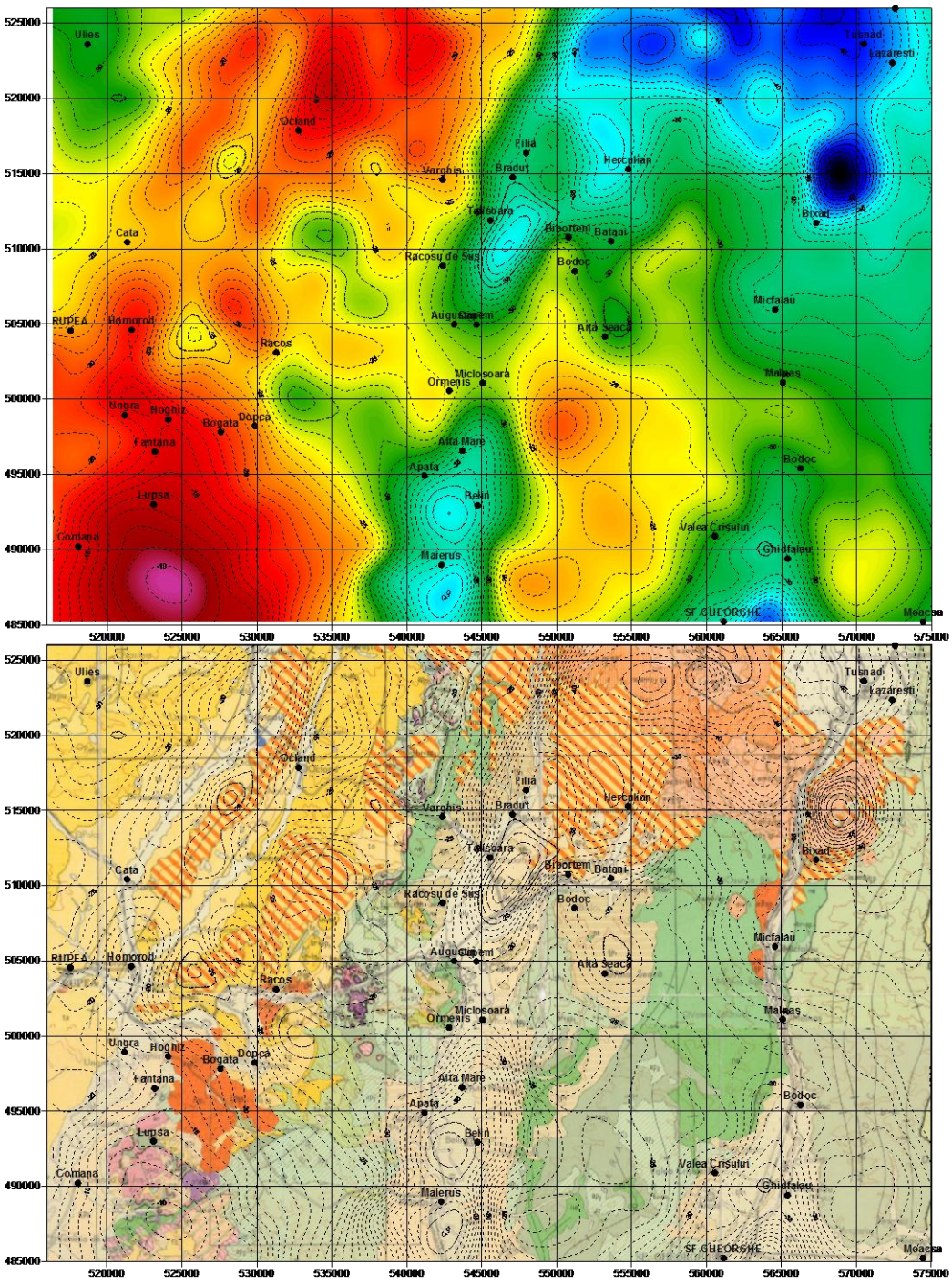

Fig. 14 - The geological model, as provided by the National Geological Map of the Romania, scale 1:200.000, and the Bouguer anomaly for the INSTEC-SUD perimeter

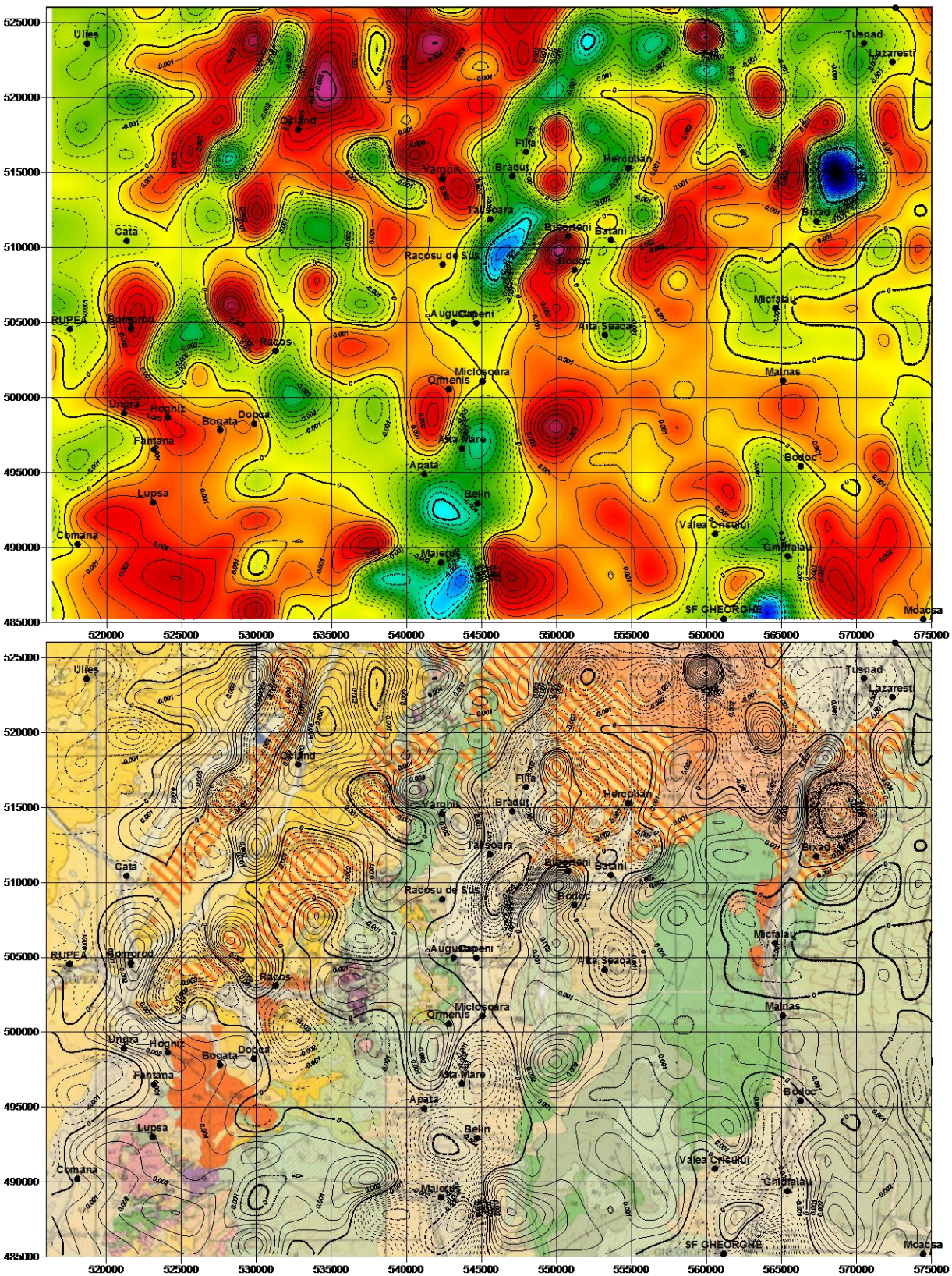

Fig. 15 - The geological model, as provided by the National Geological Map of the Romania, scale 1:200.000, and the vertical gradient of the Bouguer anomaly for the INSTEC-SUD perimeter

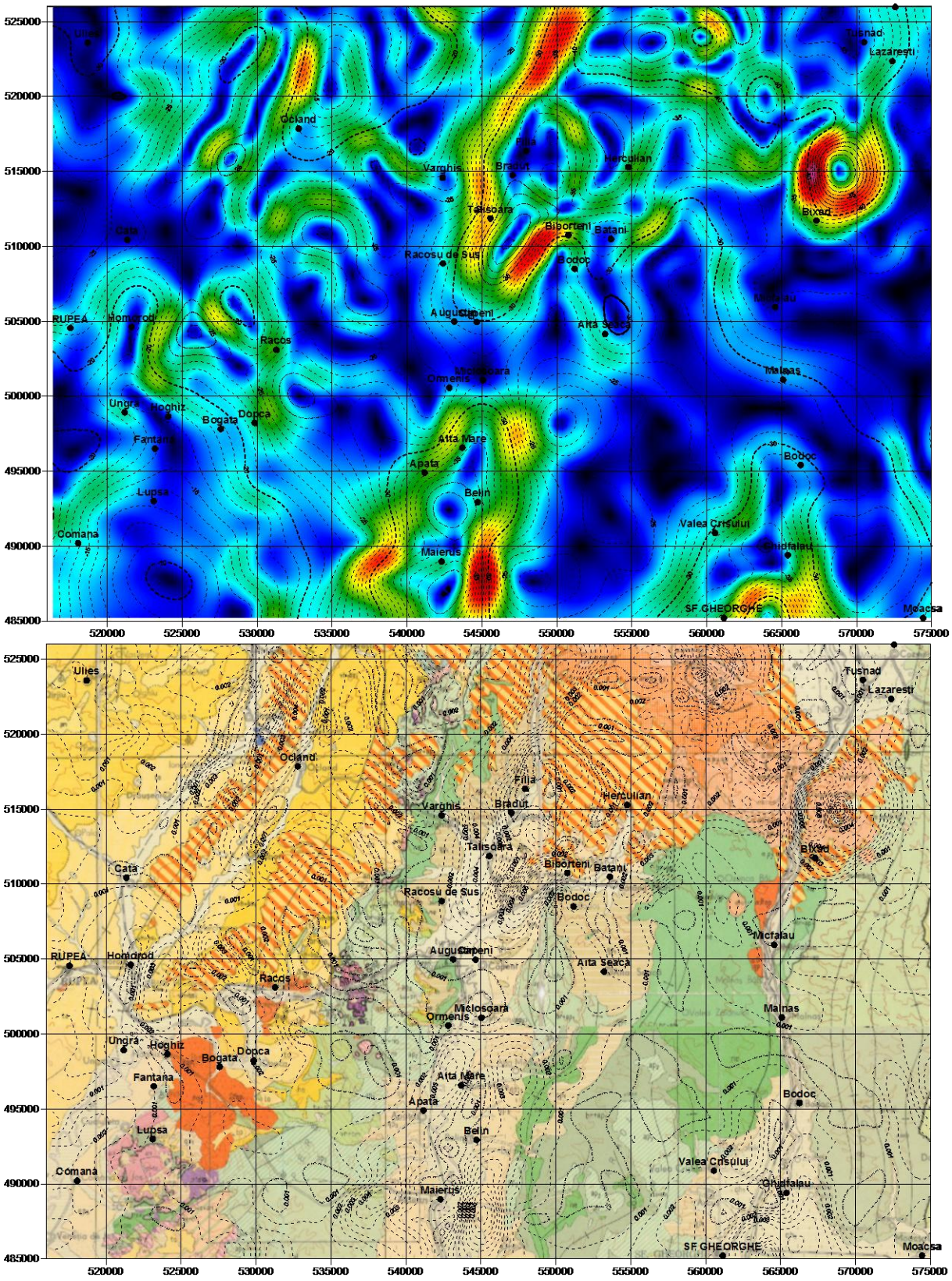

Fig. 16 - The geological model, as provided by the National Geological Map of the Romania, scale 1:200.000, and the horizontal gradient of the Bouguer anomaly for the INSTEC-SUD perimeter

(2) 2.2. GEOMAGNETIC ECHOES OF THE CURRENT GEOLOGICAL CONCEPT REGIONAL TREND

In order to analyse the imprints of the current geological models on the study area within geomagnetic data, comparative views between the geological map of the INSTEC-SUD area (as well as CIOMADUL and PERSANI sub-perimeters), and specific images of the geomagnetic field (such as total intensity scalar geomagnetic anomaly, horizontal and vertical gradients of the geomagnetic anomaly, residual geomagnetic anomaly) have been performed.

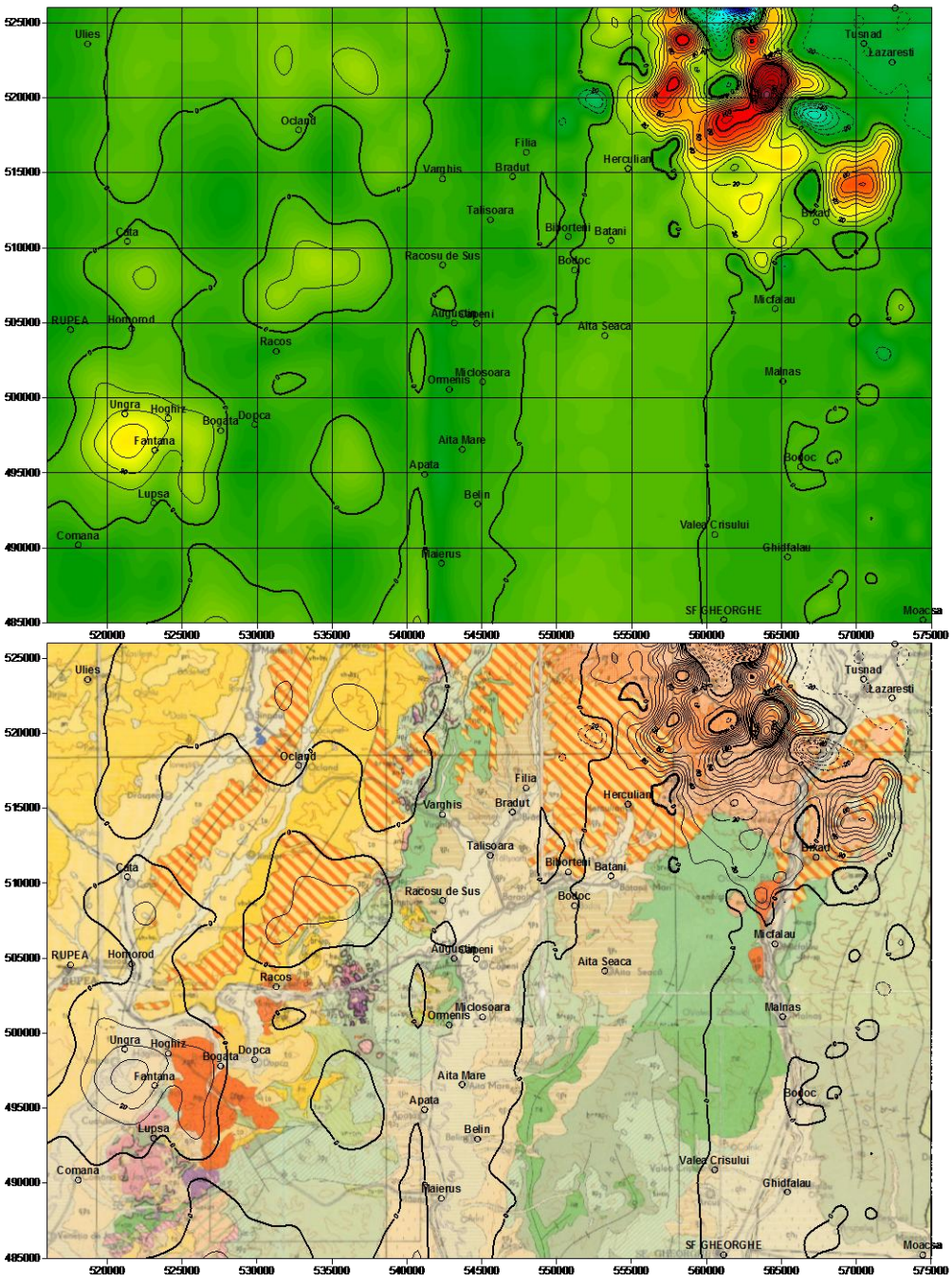

Fig. 17 - The geological model, as provided by the National Geological Map of the Romania, scale 1:200.000, and the residual geomagnetic anomaly for the INSTEC-SUD perimeter

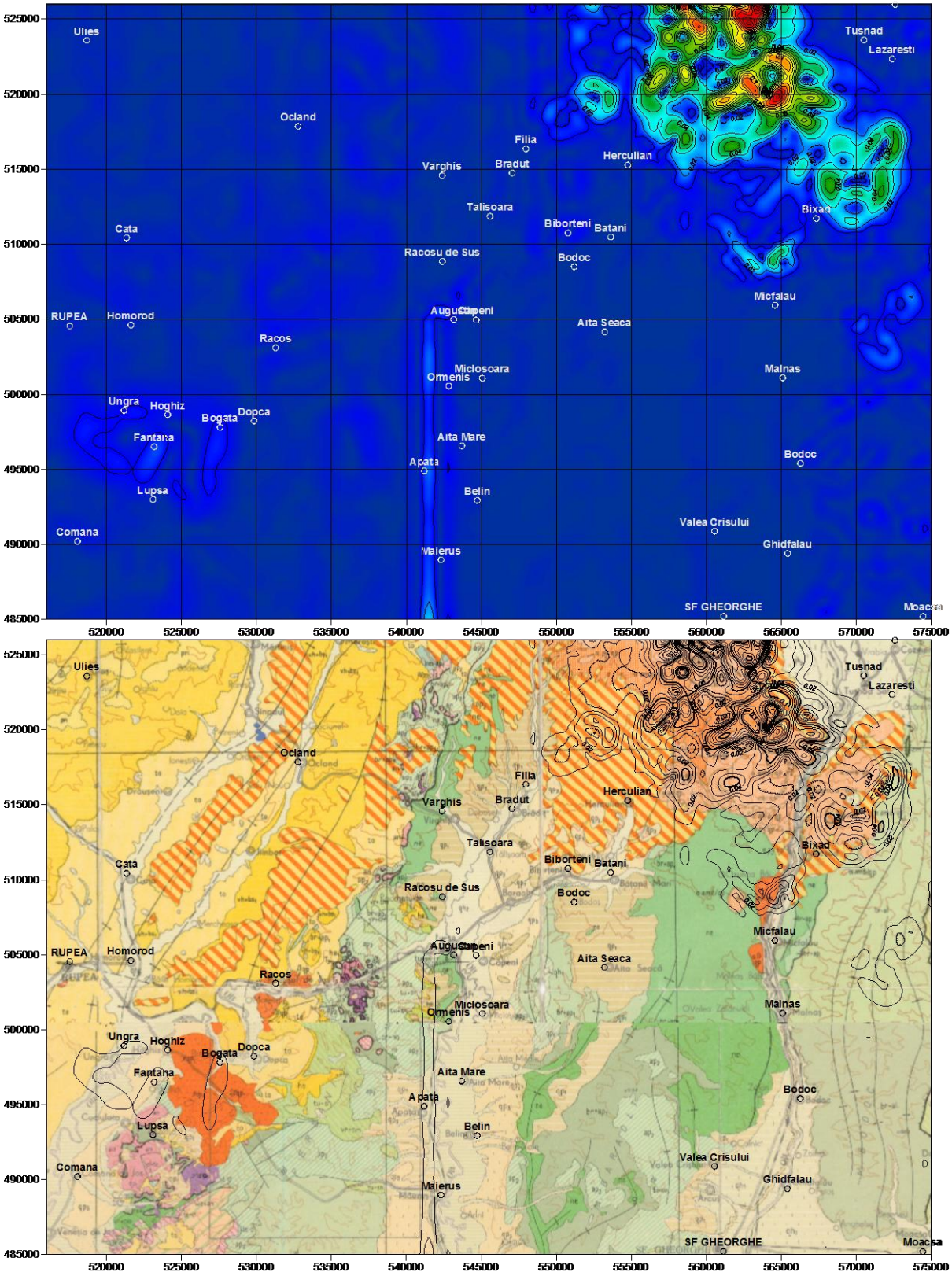

Fig. 18 - The geological model, as provided by the National Geological Map of the Romania, scale 1:200.000, and the horizontal gradient of the geomagnetic anomaly for the INSTEC-SUD perimeter

PERSANI AREA

Within the PERSANI sub-perimeter, where joint geological and geomagnetic investigations have been conducted during 2014 campaign, direct comparisons of the geological concept with the geomagnetic field pattern, but also by employing 2D numerical simulations have been performed .

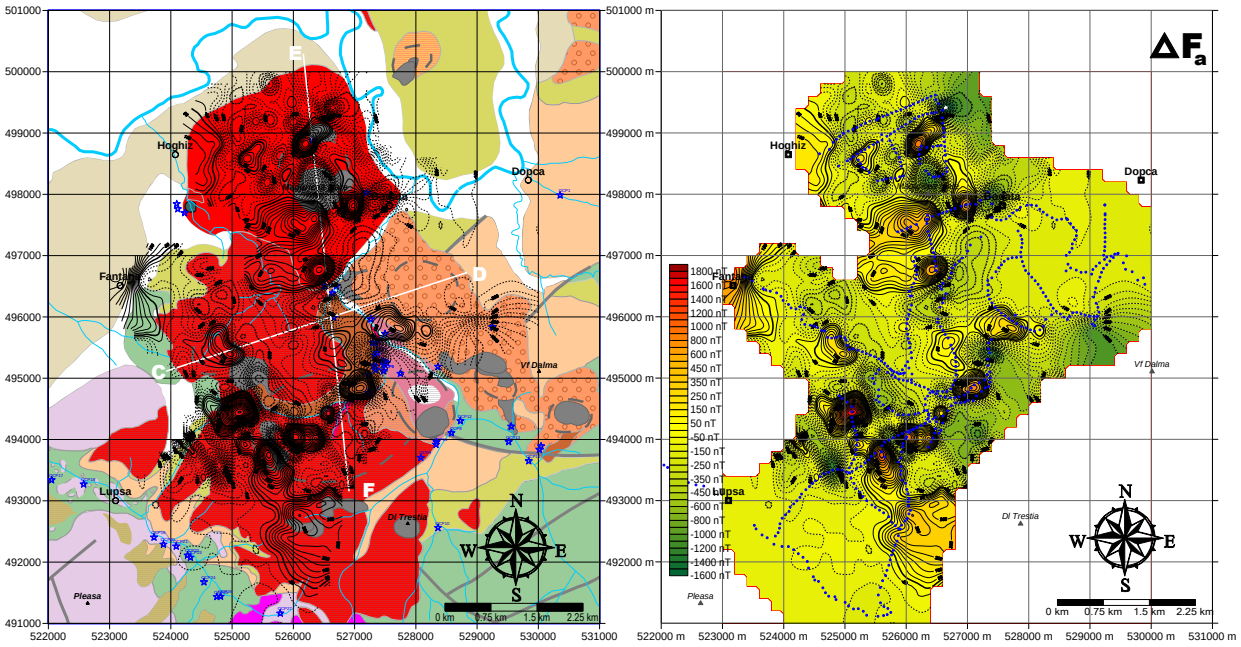

Fig. 19 - Geological model and the ground total intensity scalar geomagnetic anomaly within the PERSANI area

Comparative views are presented along the two lines crossing the investigated area.

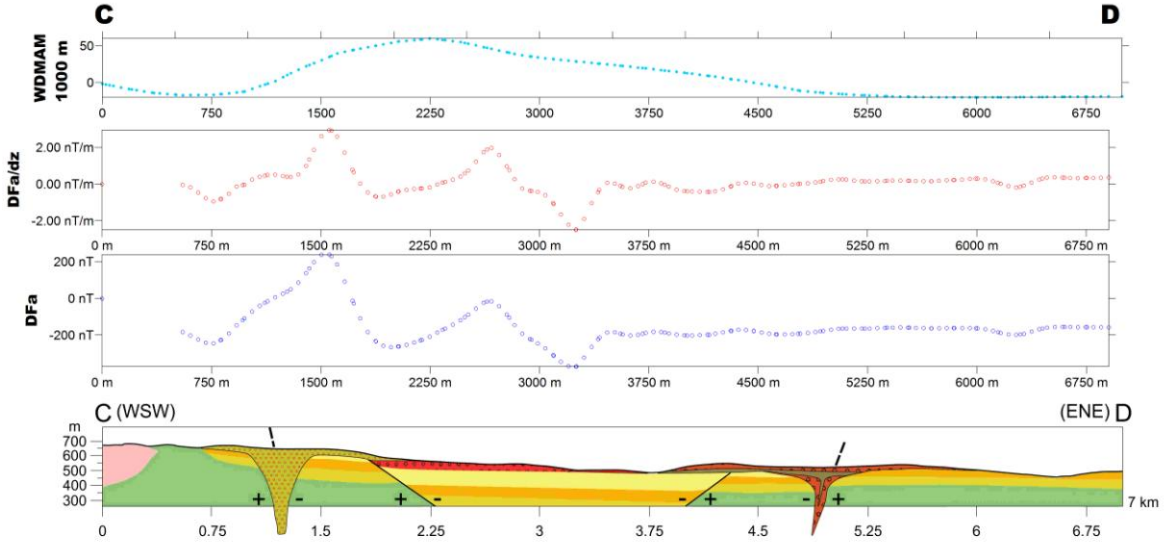

Fig. 20 - Geological model and geomagnetic data along CD line

WDMAM, geomagnetic anomaly provided by WDMAM project
DFa/dz, vertical gradient of the ground geomagnetic anomaly
DFa, ground total intensity geomagnetic anomaly

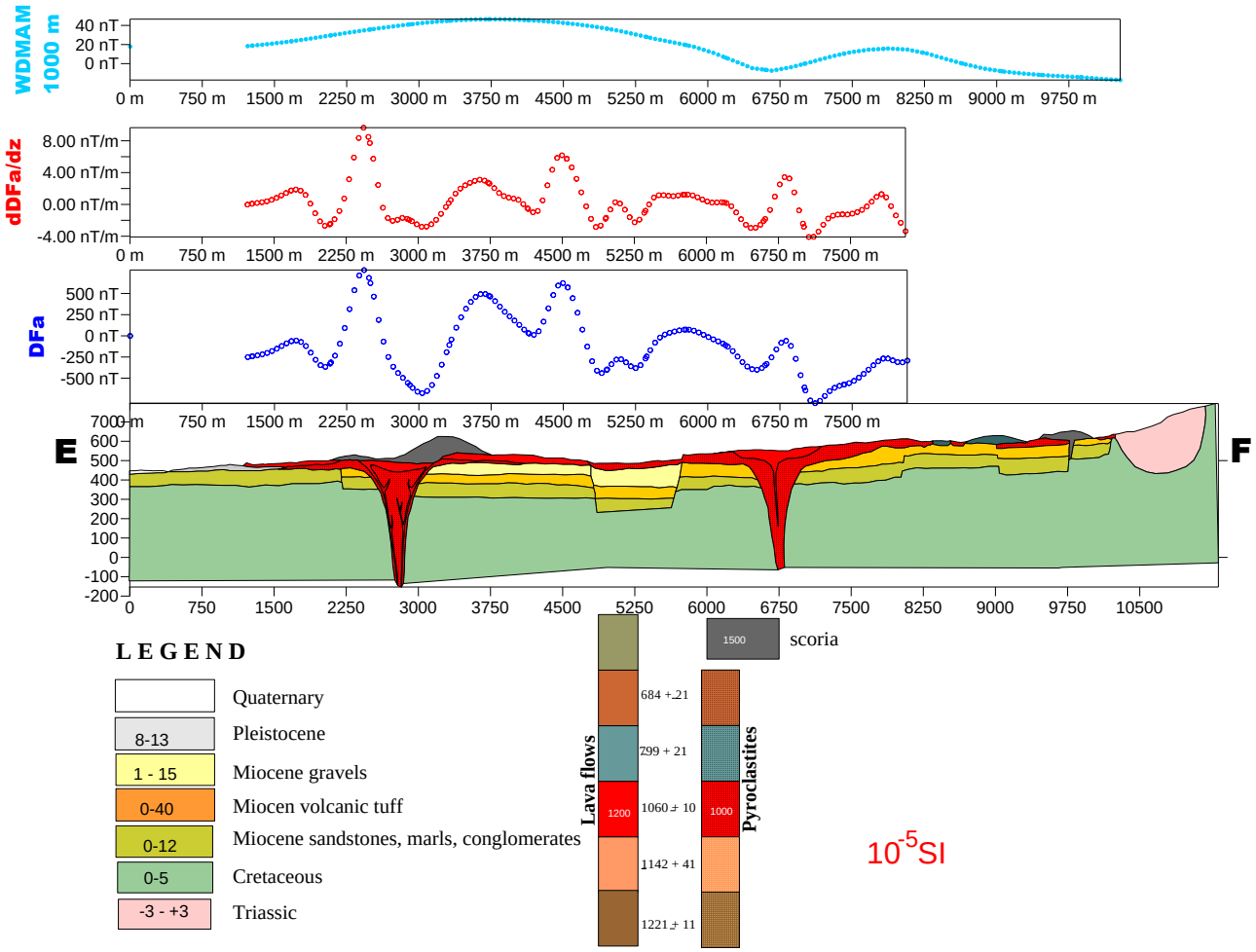

Fig. 21. Geological model and geomagnetic data along EF line

WDMAM, geomagnetic anomaly provided by WDMAM project
DFa/dz, vertical gradient of the ground geomagnetic anomaly
DFa, ground total intensity geomagnetic anomaly

Magnetic susceptibility of the main geological formations appears in the legend of the illustration (as expressed in 10^{-5} SI)

Based on the preliminary geological concept and rock physics properties of the main geological formations cropping out in the area, some tentative interpretative models of the observed geomagnetic data have been performed based on a 2D itterative approach.

As it can be seen, the final synthesized effect fits very well the observed data, offerring a good support to the revealed geological model.

The obtained results are presented in the next figure.

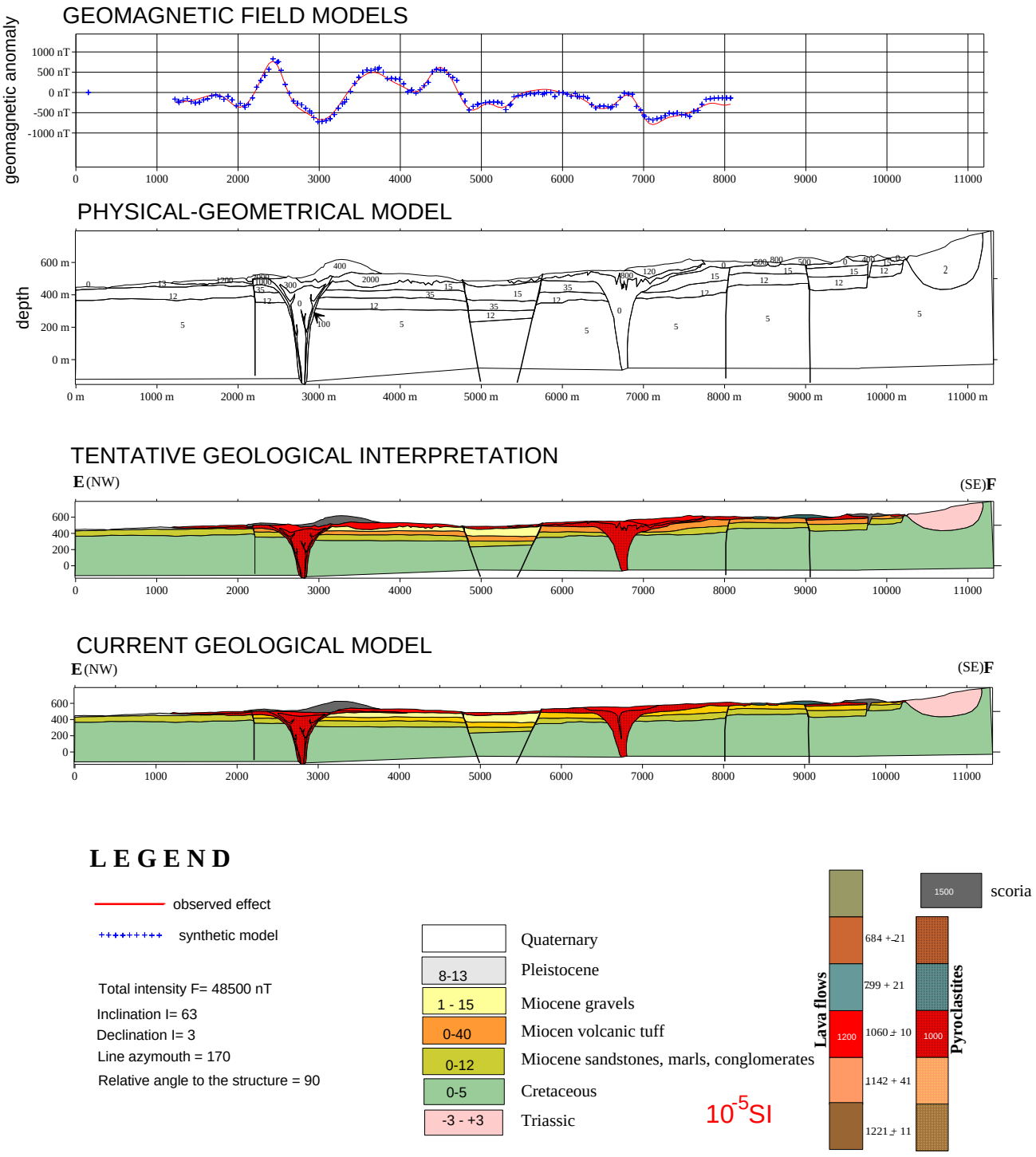

Fig. 22 - Tentative interpretative model of the geomagnetic data along the interpretative line EF within Persani area

(2) 2.3. THE ANALYSES OF THE WAY THE GEOLOGIC CONCEPT IS REFLECTED IN OTHER GEOPHYSICAL INFORMATION CATEGORIES

This activity consisted in bulding up 2D geological interpretative models along an already established profiles inside the INSTEC perimeter. Up to now, according with the field reaserch progress done between 2013-2014 we have already made two interpretative profiles (see figure 21) where we have already performed a series of detailed tectonic and petrographic observations. This profiles will be in the future the base for the geophysical interpretations that will be carried out.

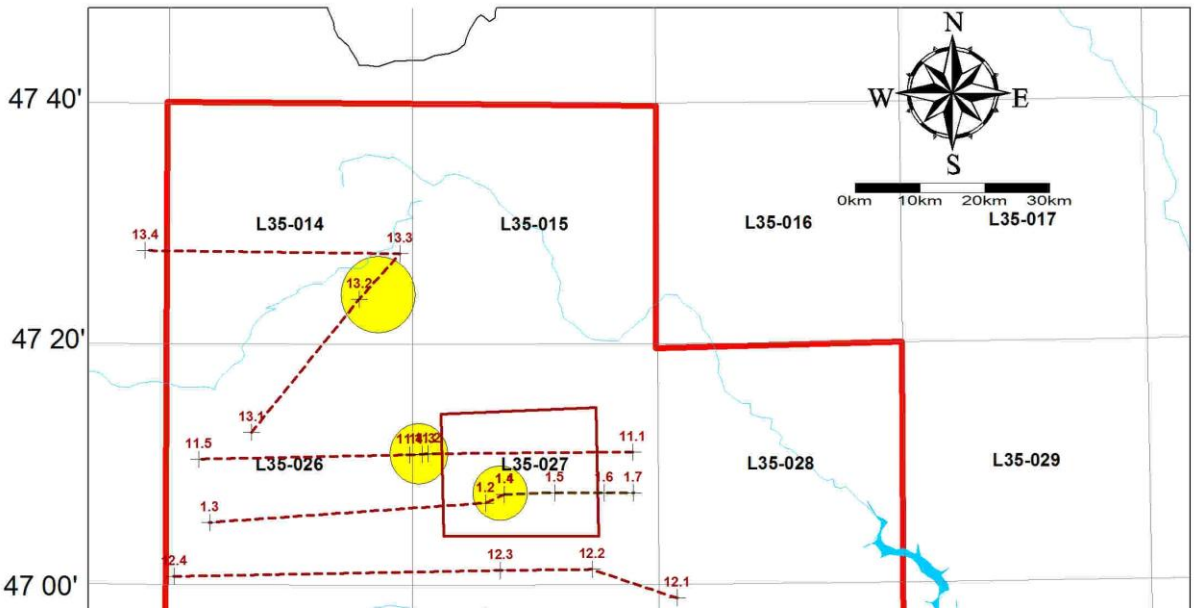

Fig. 23. **The situation and position of the interpretative profiles.**

The interpretation used all the available geological and geophysical information:

The profile 13.1-13.2 contain a common legend for the both profiles.

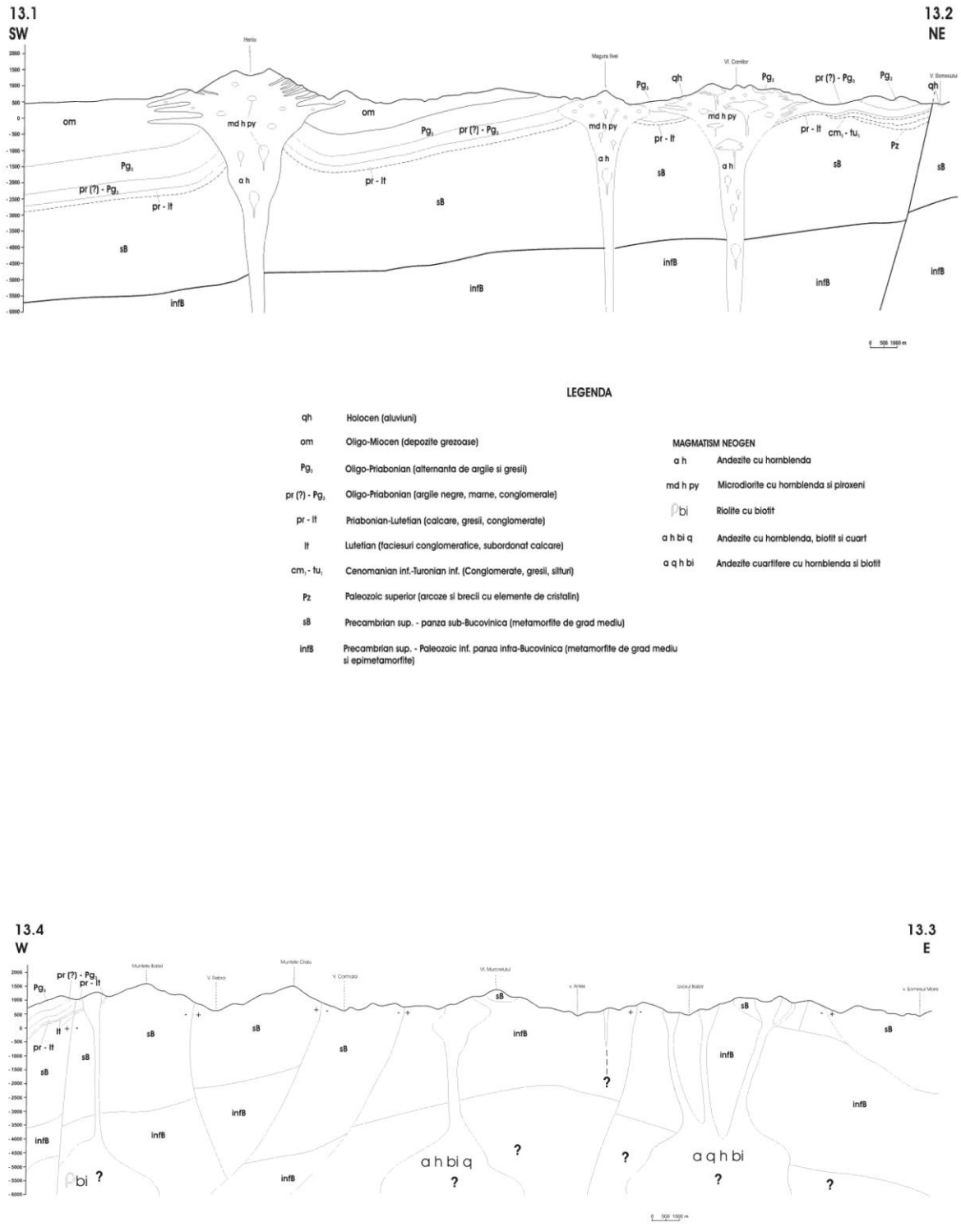

Fig. 24. **Interpretative geological profiles in the northen part of the INSTEC perimeter.**

C. FIELDWORK AND LABORATORY ACTIVITIES

(2) 3. IDENTYFING AND CHARACTERIZING THE MAIN TECTONIC ALIGNMENTS ASSOCIATED WITH MAGMATIC ACTIVITY, BASED ON GEOLOGICAL AND GEOPHYSICAL DATA (II)

(2) 3.1. INTEGRATION OF THE K/AR, PETROLOGIC AND GEOPHYSICAL DATA OF THE VOLCANIC AND SUBVOLCANIC STRUCTURES IN THE STUDY AREA

During 2014 field studies, along the complex geological observations it was finished the sampling of the main subvolcanic bodies from the Rodna-Bargau area. This sampling followed that of 2013 year. This area is situated in the northern part of the INSTEC areal.

We are showing below a table with the most important sample collection during 2013-2014 field work. The table is giving: sample code, rock type with preliminary petrographic characteristics, relative age of the rocks in Ma, according to the Pécskay et al. (2009), GPS position of the samples, along with the density calculated in the our geophysical lab. The samples have been recently chemically analysed in a cooperation with Neaples University, with whom we established a bilateral agreement. In the next stage the geochemical and petrographic data will be processed.

Cod roca	**Rock type petrografie**	**Age (Ma) K/Ar data**	**LAT grades**	**LATm minutes**	**LONG grades**	**LONGm minutes**	**ALT (m)**	**dens (g/cmc**	**Cod GPS**
FLN-1	riolite	8	47	26.854736	24	31.157009	885	2.50	423
FLN-1A	riolite	8	47	26.854736	24	31.157009	885	2.63	423
FLN-2	riolite	8	47	21.109925	24	31.964809	847	2.34	424
FLN-3B	dacite	10.8	47	22.783994	24	41.475729	475	2.66	425
FLN-4	bazaltic andesite	8.5	47	24.647075	24	41.331746	597	2.7	426
FLN-5	andesite	10.3	47	24.681033	24	41.608101	619	2.62	427
FLN-6	andesite	9	47	24.735712	24	42.917781	899	2.57	428
FLN-7	andesite	10	47	24.861494	24	42.541181	863	2.61	429
FLN-8	andesite	10.1	47	24.691800	24	41.734800	652	2.58	-
FLN-9	andesite	9	47	24.560177	24	40.667515	525	2.62	430

FLN-10	dacite	10.8	47	24.907736	24	40.346060	533	2.44	431
FLN-11	dacite	10.8	47	24.240650	24	38.792470	601	2.52	432
FLN-12	dacite	10.8	47	24.384356	24	38.780118	626	2.51	433
FLN-12B	hornfels	10.8	47	24.384356	24	38.780118	626	2.55	433
FLN-13	dacite	10.7	47	24.187238	24	37.946212	651	2.49	434
FLN-14	dacite	8	47	25.051970	24	47.664307	522	2.64	435
FLN-15	andesite	8.7	47	20.499388	24	43.264256	473	2.57	436
FLN-16	dacite	9	47	21.426943	24	44.134514	497	2.55	437
FLN-18	dacite	9.5	47	22.488710	24	45.272822	505	2.59	438
FLN-19	microdiorite	9.5	47	22.725151	24	45.375826	516	2.64	439
FLN-20	andesite	9.4	47	22.905731	24	46.316756	533	2.57	440
FLN-21	dacite	10	47	22.873369	24	46.701169	538	2.52	441
FLN-22	basaltic andesite	8.8	47	22.663186	24	47.735121	554	2.61	442
FLN-23	microdiorite	9.8	47	22.364833	24	49.384894	648	2.51	443
FLN-24	microdiorite	9.7	47	22.570468	24	49.357396	589	2.75	444
FLN-25	microdiorite	9.7	47	22.622906	24	50.427016	637	2.65	445
FLN-26	andesite	9.5	47	21.829229	24	53.328724	626	2.72	446
FLN-27	andesite	9.6	47	24.752653	24	55.545175	746	2.55	447
FLN-28	andesite	8	47	27.686015	24	49.219800	600	2.53	448
FLN-29	andesite	8	47	28.598633	24	49.790590	665	2.55	449
FLN-30	andesite	8	47	28.342981	24	49.373428	678	2.65	450
FLN-32	andesite	9.4	47	26.081293	24	48.555167	553	2.69	451
FLN-33	microdiorite	9.1	47	26.002652	24	53.058583	652	2.71	453
FLN-34	andesite	8	47	25.446000	24	52.765800	660	2.54	-
FLN-34A	andesite	8	47	25.446000	24	52.765800	660	2.72	-
FLN-35	andesite	8	47	26.974247	24	41.757649	760	2.62	454
FLN-36	andesite	8	47	26.772215	24	41.379299	715	2.67	455
FLN-37	andesite	9.3	47	20.509370	24	54.000850	708	2.73	456
FLN-37A	andesite	9.4	47	20.509370	24	54.000850	708	2.66	456
FLN-38	basaltic andesite	8.5	47	20.425109	24	54.261560	735	2.58	457

FLN-39	sandstone	30	47	24.836099	24	54.854929	705	2.58	458
FLN-40	andesite	9.7	47	16.028782	24	41.943322	729	2.7	459
FLN-41	andesite	9.5	47	15.988619	24	42.010700	758	2.67	460
FLN-42	andesite	9.5	47	15.754346	24	41.897368	889	2.7	461
FLN-43	andesite	9.8	47	17.068234	24	42.832171	960	2.68	462
FLN-44	andesite	9.5	47	17.103544	24	42.773020	946	2.67	463
FLN-45	andesite	9.5	47	16.088525	24	42.103395	808	2.68	464
FLN-46	andesite	9.5	47	16.132175	24	42.327583	811	2.62	465
FLN-47	andesite	10.4	47	12.787576	24	53.002889	704	2.64	466
FLN-48	andesite	10.5	47	14.130143	25	0.322025	1099	2.64	467
FLN-49	andesite	10.1	47	15.855155	25	1.423620	1196	2.69	468
FLN-50	andesite	9.4	47	14.124549	24	0.085386	1053	2.71	469
FLN-51	andesite	10.5	47	13.656426	24	58.407016	936	2.69	470
FLN-52	andesite	9.5	47	13.387787	24	55.486790	805	2.69	471
FLN-53	andesite	10.2	47	13.224778	24	55.303761	827	2.63	472
FLN-54	andesite	9.6	47	23.621097	25	9.203057	918	2.28	473
FLN-55	andesite	9.6	47	23.105376	25	9.930778	901	2.63	474
FLN-56	andesite	9.8	47	12.949636	25	5.012069	1041	2.69	475
FLN-57	andesite	10	47	12.906991	25	5.285219	1070	2.7	476
FLN-58	diorite	10.2	47	8.776041	25	6.408961	1230	2.75	477
FLN-59	andesite	10	47	10.028739	25	5.187203	1179	2.66	478
FLN-60	andesite	9.9	47	10.149902	25	5.377488	1159	2.67	479
FLN-61	andesite	10	47	10.734853	25	5.357942	1120	2.64	480
FLN-62	andesite	10	47	16.294126	25	5.598596	997	2.81	481
FLN-63	riolite	8.8	47	17.342400	25	12.977400	990	2.53	-
FLN-64	andesite	9.8	47	16.889756	25	12.099540	1024	2.6	482
FLN-65	andesite	9.8	47	16.889756	25	12.099540	1024	2.61	482
FLN-66	andesite	9.8	47	14.442955	25	10.445890	1117	2.68	483
FLN-67	andesite	9.8	47	14.835147	25	10.809375	1153	2.68	484
FLN-68	andesite	9.8	47	15.115724	25	10.435439	1102	2.56	485
FLN-69	andesite	9.8	47	18.812004	25	13.537029	934	2.64	486

FLN-70	basaltic andesite	9.4	47	13.879497	24	57.534935	1006	2.69	487
FLN-71	andesite	9.7	47	13.396467	24	53.289405	976	2.62	488
FLN71A	andesite	9.8	47	13.184725	24	53.508984	832	2.68	489
FLN-72	andesite	10	47	12.513827	24	56.085061	1303	2.75	490
FLN-73	andesite	10.1	47	12.337886	24	55.227765	1178	2.69	491
FLN-74	andesite	9.8	47	12.793842	24	54.905232	1074	2.62	492
FLN-75	andesite	9.8	47	12.96788	24	55.117184	1023	2.68	493
FLN-76	andesite	9.8	47	16.212583	25	5.7704328	981	2.72	494
FLN-77	dacite	9	47	14.715542	25	7.3471128	1182	2.31	495
FLN-78	andesite	9.6	47	15.02288	24	58.393045	965	2.68	496
FLN-79	microdiorite	9.9	47	15.865512	24	55.000719	805	2.71	497
FLN-80	andesite	9.7	47	17.188662	24	54.153661	796	2.75	498
FLN-81	andesite	9.7	47	18.470629	24	51.509569	664	2.59	499
FLN-82	andesite	9.7	47	10.532619	24	56.112905	964	2.67	500
FLN-83	andesite	9.7	47	10.595084	24	55.864519	935	2.59	501
FLN-84	microdiorite	10.2	47	10.310923	25	3.0981882	1000	2.9	502
FLN-85	microdiorite	10.2	47	10.49477	25	2.7518142	1174	2.77	503
FLN-86	microdiorite	10.2	47	16.883649	24	47.469444	792	2.7	504
FLN-87	andesite	9.6	47	17.482846	24	47.269279	707	2.71	505
FLN-88	andesite	9.7	47	17.680527	24	45.151937	653	2.72	506
FLN-89	andesite	9.7	47	18.79321	24	44.364825	507	2.73	507
FLN-90	andesite	9.7	47	18.906177	24	44.060754	490	2.7	508
FLN-91	andesite	9.8	47	24.061052	24	53.954309	1002	2.6	-
FLN-92	andesite	9.9	47	24.563043	24	54.366323	826	2.7	-
474	sandstone	30	47	23.105376	25	9.9307776	901	2.61	474
FLN-59C	andesite	10	47	10.028739	25	5.1872034	1179	2.44	478
FLN-64S	clay	30	47	28.149594	25	20.1659	1024	2.48	482
71A1	sandstone	30	47	13.184725	24	53.508984	976	2.99	488
71S	sandstone	30	47	13.184725	24	53.508984	976	2.57	488
87S1	sandstone	30	47	17.482846	24	47.269279	707	2.55	505

87S2	sandstone	30	47	17.482846	24	47.269279	707	2.4	505
87S3	clay	30	47	17.482846	24	47.269279	707	2.17	478
FLN-59B	sandstone	30	47	10.028739	25	5.1872034	1179	2.55	478
64S1	sandstone	30	47	28.149594	25	20.1659	1024	2.46	482

Below we show a geological map (1:200.000, IGR) with the GPS points of the collected samples (according to the GPS code in the table).

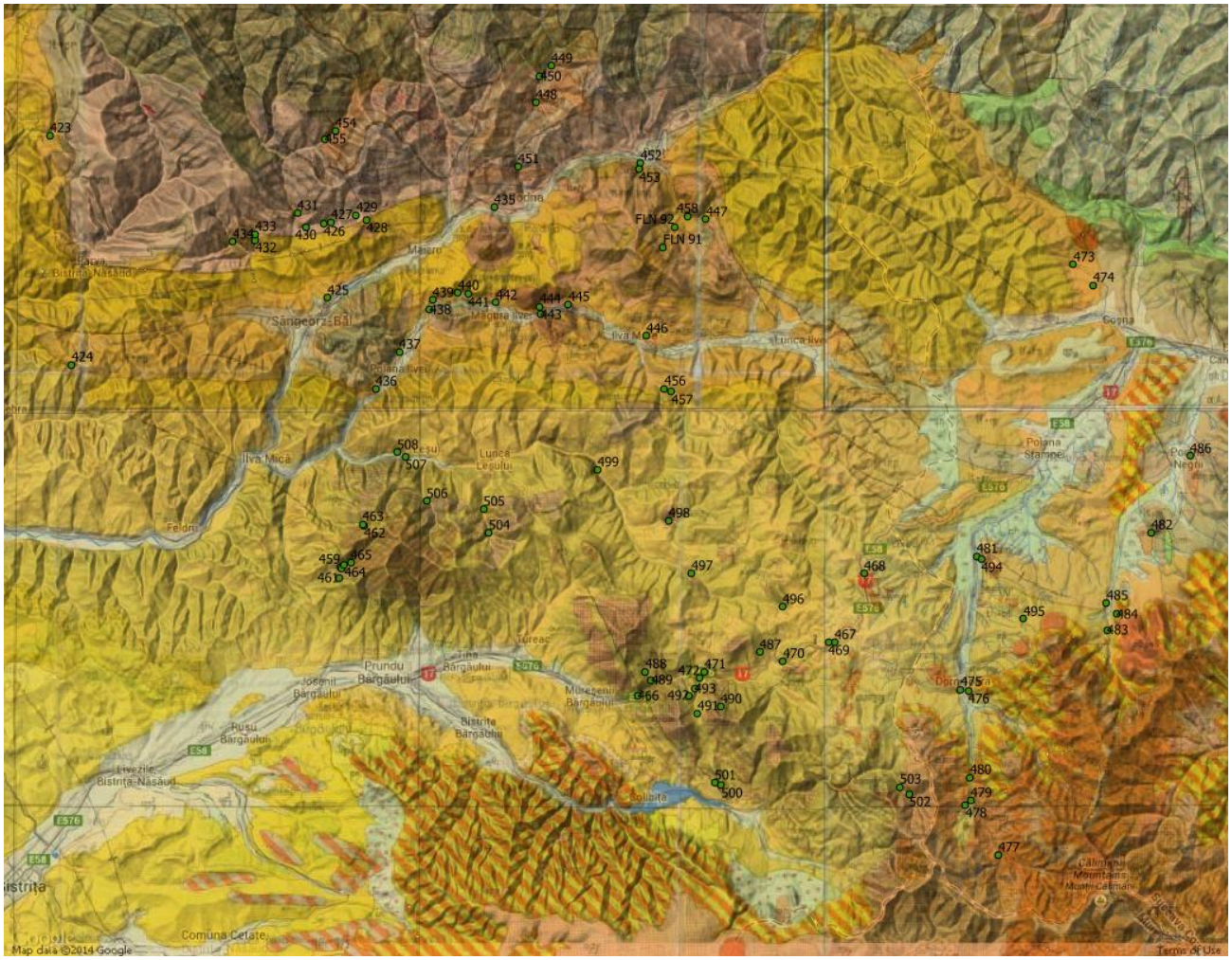

Fig. 25 - **Location of the subvolcanic rock samples collected during 2013-2014 field work campains.**

(2) 3.2. FIELD AND LABORATORY ACTIVITIES FOR NEW GEOLOGICAL AND GEOPHYSICAL DATA AQUISITION IN ORDER TO SOLVE THE RELATIONSHIP BETWEEN TECTONIC AND VOLCANIC STRUCTURAL FEATURES. ROCK SAMPLING FOR SPECIFIC GEOCHEMICAL AND PETROPHYSICAL ANALYSES (I).

(2) 3.2.1. GEOLOGICAL INVESTIGATIONS

The results geological observations obtained during the field campaign have allowed the construction two detailed maps for the southern part of the INSTEC perimeter.

It is about the new geological map of Ciomadul volcano and Persani Mts. alkali basaltic volcanism. The Persani Mts new volcanologic map is shown along the geophysical interpretations in Fig. 19.

We show below a new simplified 3D map of Ciomadul volcano (fig. 24), showing also the published and unpublished K/Ar data that will be published soon in an international journal along with volcanological interpretations:

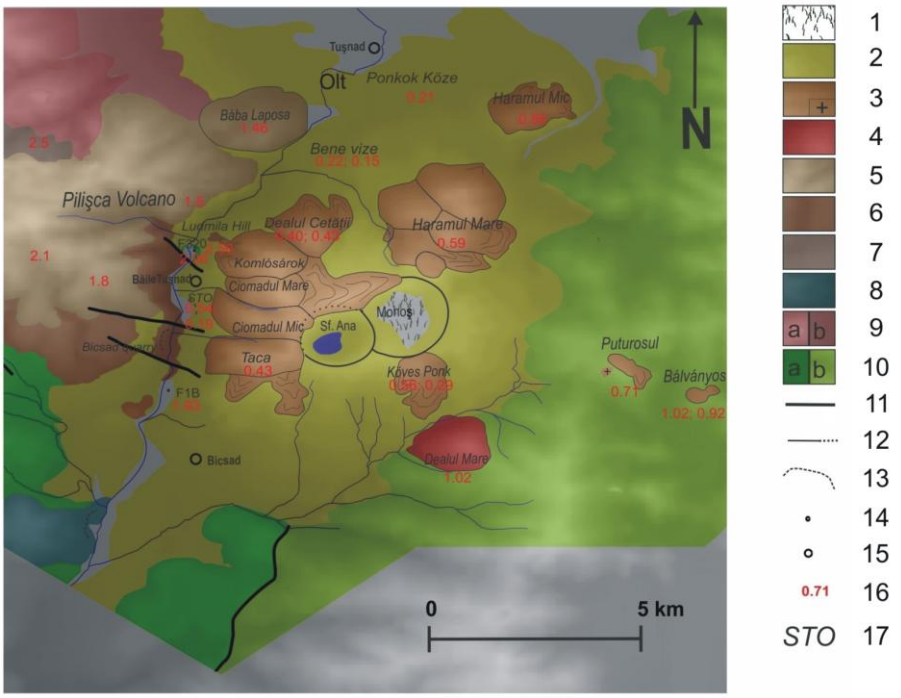

Geological map of Ciomadul volcano. Legend: 1. Mohoş swamp; 2. Ciomadul volcano - volcaniclastic deposits; 3. Ciomadul dacite domes-; +: intrusion; 4. Andesite dome (Dealul Mare); 5. Pilişca volcano - andesite and dacite domes; 6. Pilişca volcano -andesite with amphibole and pyroxene; 7. Pilişca volcano - basaltic andesite (Mitaci type); 8. Shoshonite (Murgul Mic dome); 9. Cucu volcano: a. andesite with amphibole ± biotite; b. volcaniclastic deposits; 10. Cretaceous flysch deposits: a. Tithonic-Neocomian; b. Barremian-Albian; 11. Faults; 12. Crater outline; 13 Quarry; 14. Drilling; 15. Town; 16. K-Ar age; 17. STO-South Tuşnad Outcrop.

Fig. 26.

(2) 3.2.2. GEOPHYSICAL INVESTIGATIONS

During the second stage, geophysical research have been conducted into two main directions:
- field observations
- lab determinations and data processing

FIELD GEOPHYSICAL ACTIVITIES

New data acquisition have been performed in order to complement the current information and to advance the state-of-the-art knowledge in the investigated area.

As long as the National Agency for Mineral Resources denies the access to the previously obtained information, the role of data acquisition in the project has been considerably increased.

Many areas previously covered by geophysical observations had to be re-surveyed, increasing resources spent for field activities in the detriment of data processing and interpretation.

The much more extended surface to be covered by field activities has determined a thorough planning of the areas to be surveyed each year of the project. The specific scheduling is presented in the next figure.

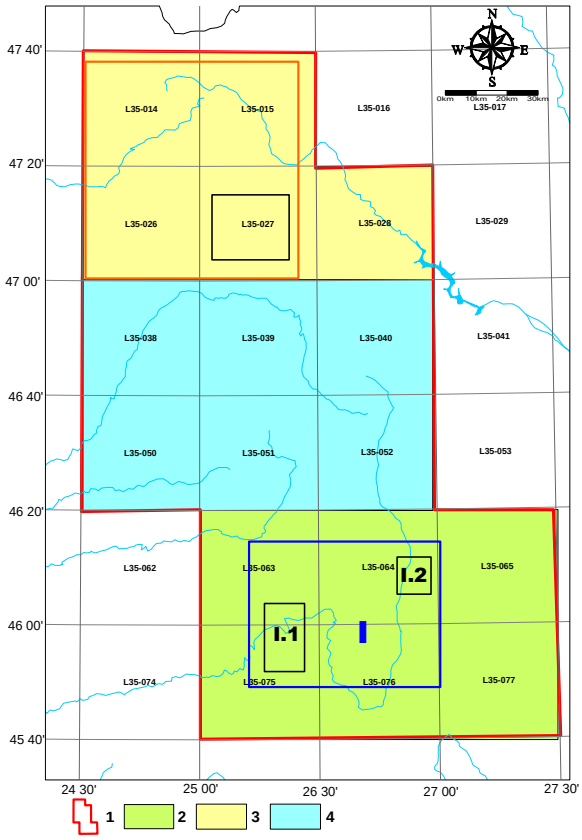

Fig. 27 - SCHEDULING FIELD SURVEYS WITHIN THE INSTEC PROJECT

1, INSTEC overall perimeter; 2, area covered during 2014 field campaign; 3, planned works during 2015 field campaign; 4, area to be covered during 2016
I, INSTEC-SUD perimeter; I.1, Perşani sub-perimeter; I.2. Ciomadu sub-perimeter

From the methodological point of view, research performed can be grouped into:

- gravity survey
- ground magnetics

GRAVITY SURVEYS

Gravity observations has been performed by employing a Canadian gravity meter Scintrex CG-5 AUTOGRAV (1 microgal accuracy).

a) preparative activities: consisted of checking-out operations for gravity scale and drift factor

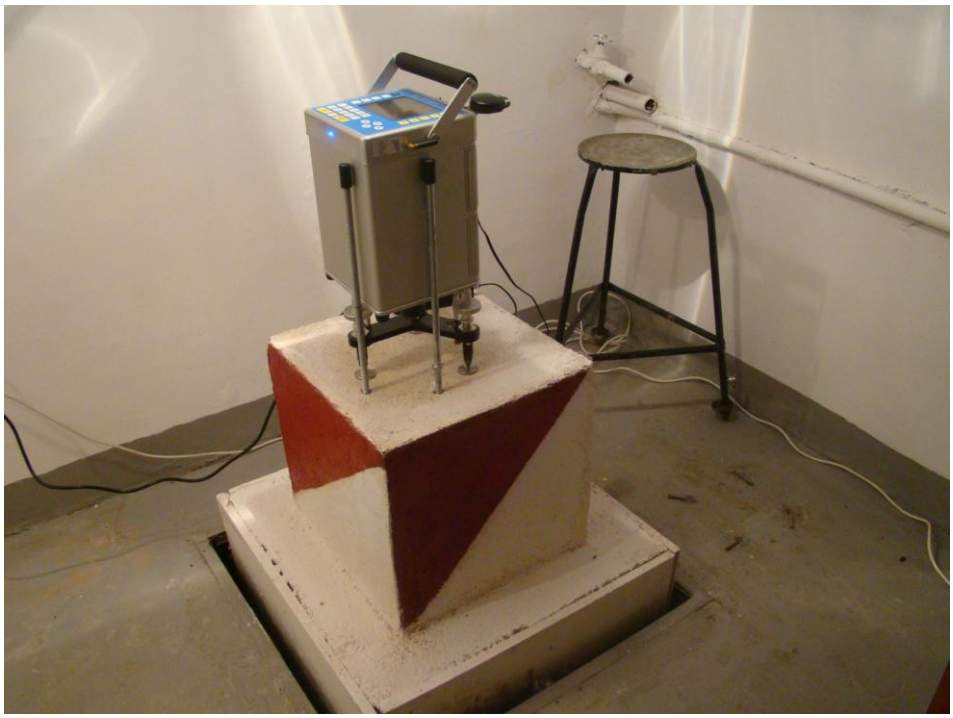

Fig. 28 - CG-5 AUTOGRAV METER OPERATED IN THE SEDD GRAVITY LAB FOR DRIFT FACTOR DETERMINATION

b) observations on the gravity reference network for transferring absolute gravity values

Fig. 29 - CG-5 AUTOGRAV METER OPERATED ON THE P116-SANZIENI (TG. SECUIESC) PILLAR OF THE GRAVITY REFERENCE NETWORK

c) current survey in the study area

Fig. 30 - CG-5 AUTOGRAV METER OPERATED IN THE CENTRAL BASE-STATION OF THE 2014 SURVEY: LEPSA FROM THE 2nd ORDER GRAVITY NETWORK OF ROMANIA

Fig. 31 - CG-5 AUTOGRAV METER OPERATED IN A CURRENT STATION IN THE FIELD

GROUND MAGNETICS

Geomagnetic field observations have been performed by using two types of instruments own by the Solid Earth Dynamics Department (SEDD):

a) proton magnetometer Geometrics G856 AX (10^{-9} T accuracy) - usually employed in current field survey

Fig. 32 - MAGNETICS TEAM OPERATING THE G856 AX IN THE DOPCA BASE-STATION

B) optical-pump magnetometer Scintrex SM-5 NAVMAG (10^{-12} T accuracy) mainly employed for the determination of the effect of the external sources of the geomagnetic field.

FIG. 33 - SCINTREX SM-5 NAVMAG OPERATED FOR DIURNAL ACTIVITY SERVICE

MAIN RESULTS

The results obtained during the field campaign have allowed the construction of several models of the gravity/geomagnetic field in the study area such as:

- regional-scale geomagnetic images for INSTEC-SUD area
- semi-detailed images were obtained for the CIOMADU and PERSANI sub-perimeters

REGIONAL-SCALE IMAGES

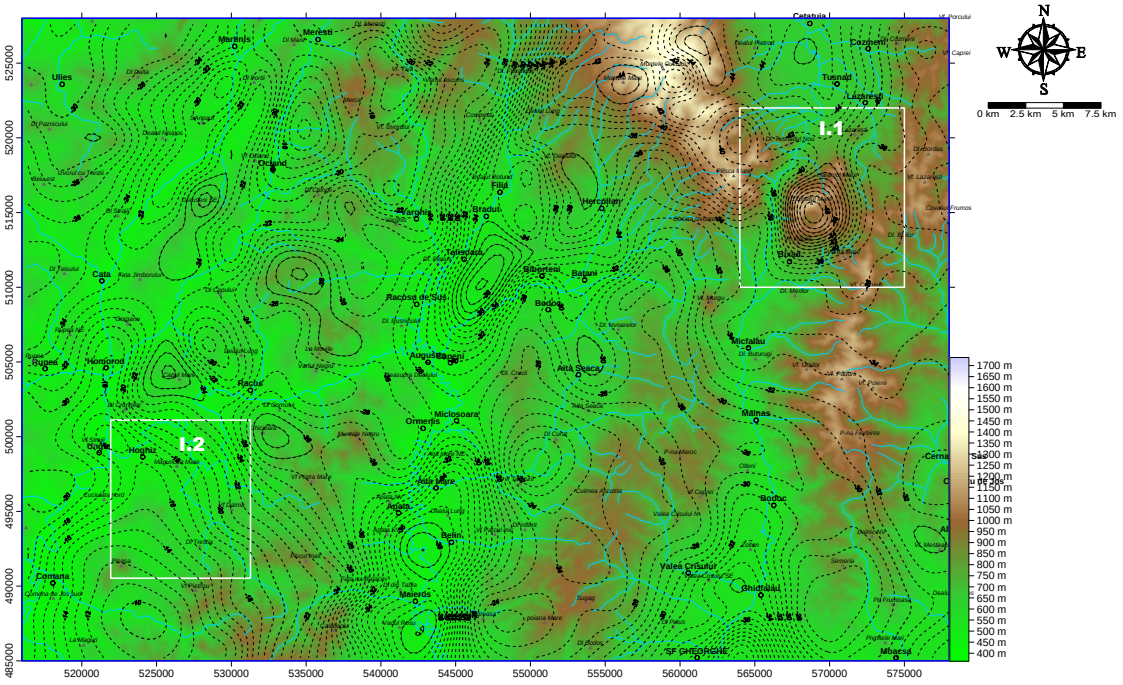

Fig. 34 - INSTEC-SUD: Bouguer anomaly for a reference density of 2.67 g/ccm

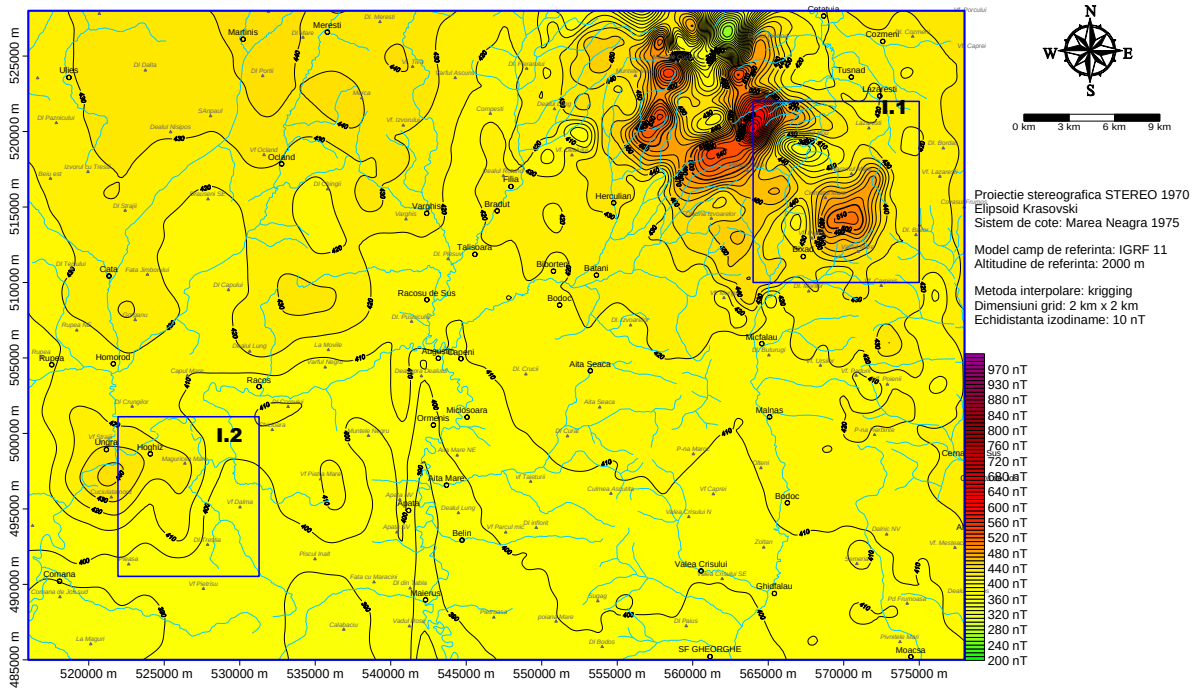

Fig. 35 - INSTEC-SUD: Total intensity scalar geomagnetic anomaly on a plan located at 2000 m altitude

LOCAL-SCALE IMAGES

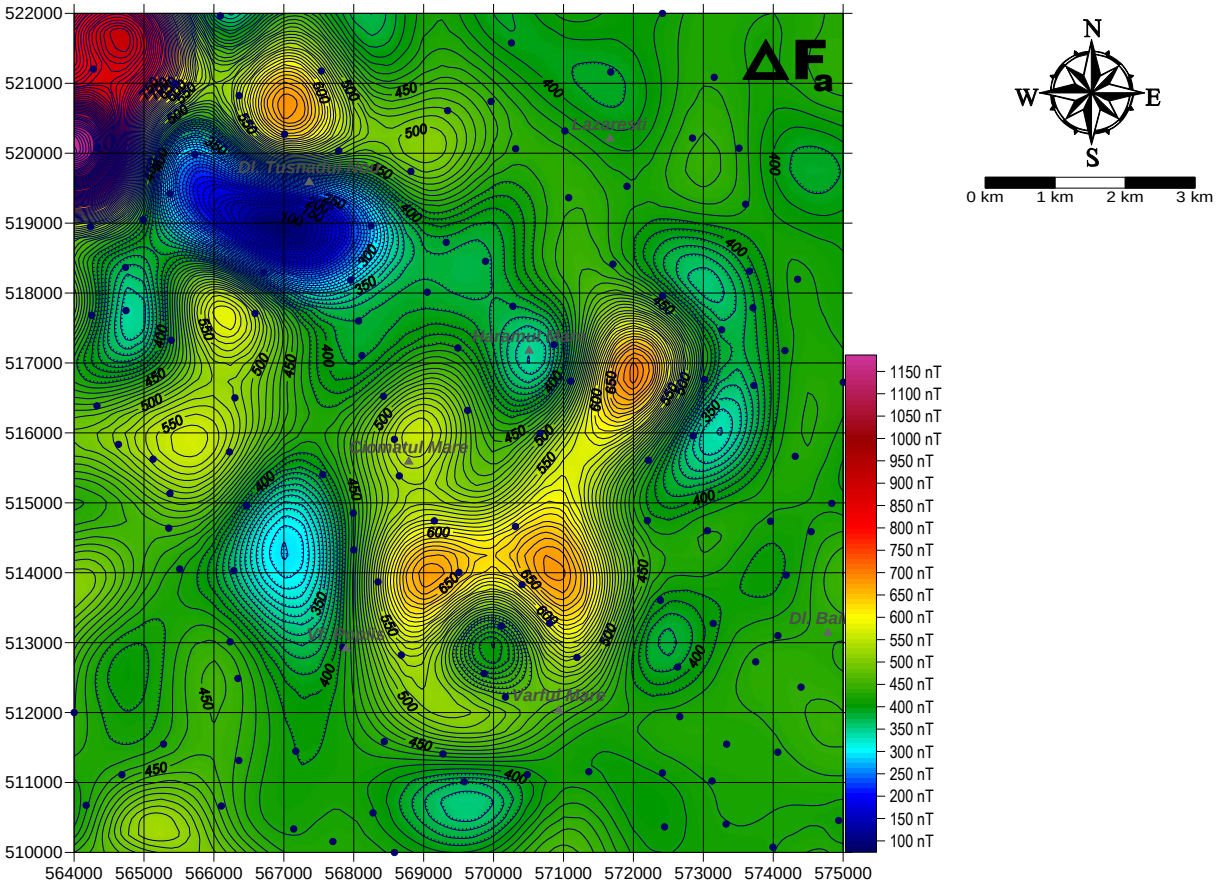

Fig. 36 - CIOMADUL AREA: Total intensity scalar geomagnetic anomaly on a plan located at 1000 m altitude

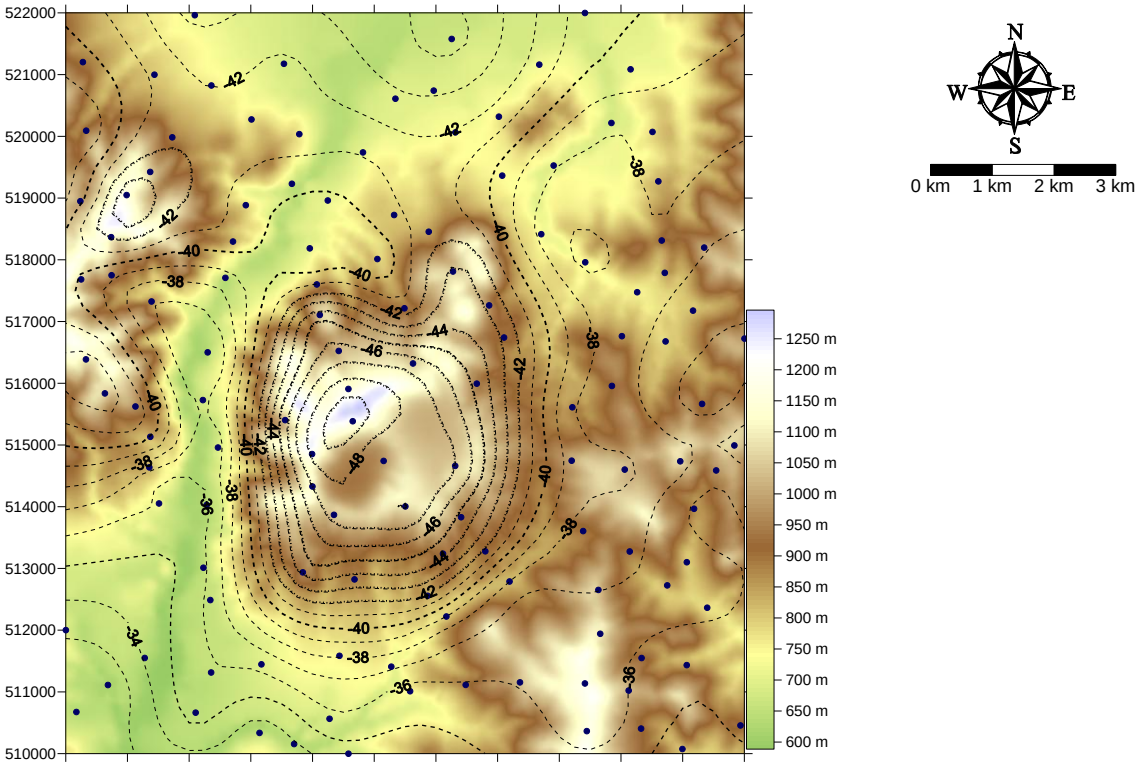

Fig. 37 - CIOMADUL AREA: Bouguer anomaly for a reference density of 2.67 g/ccm

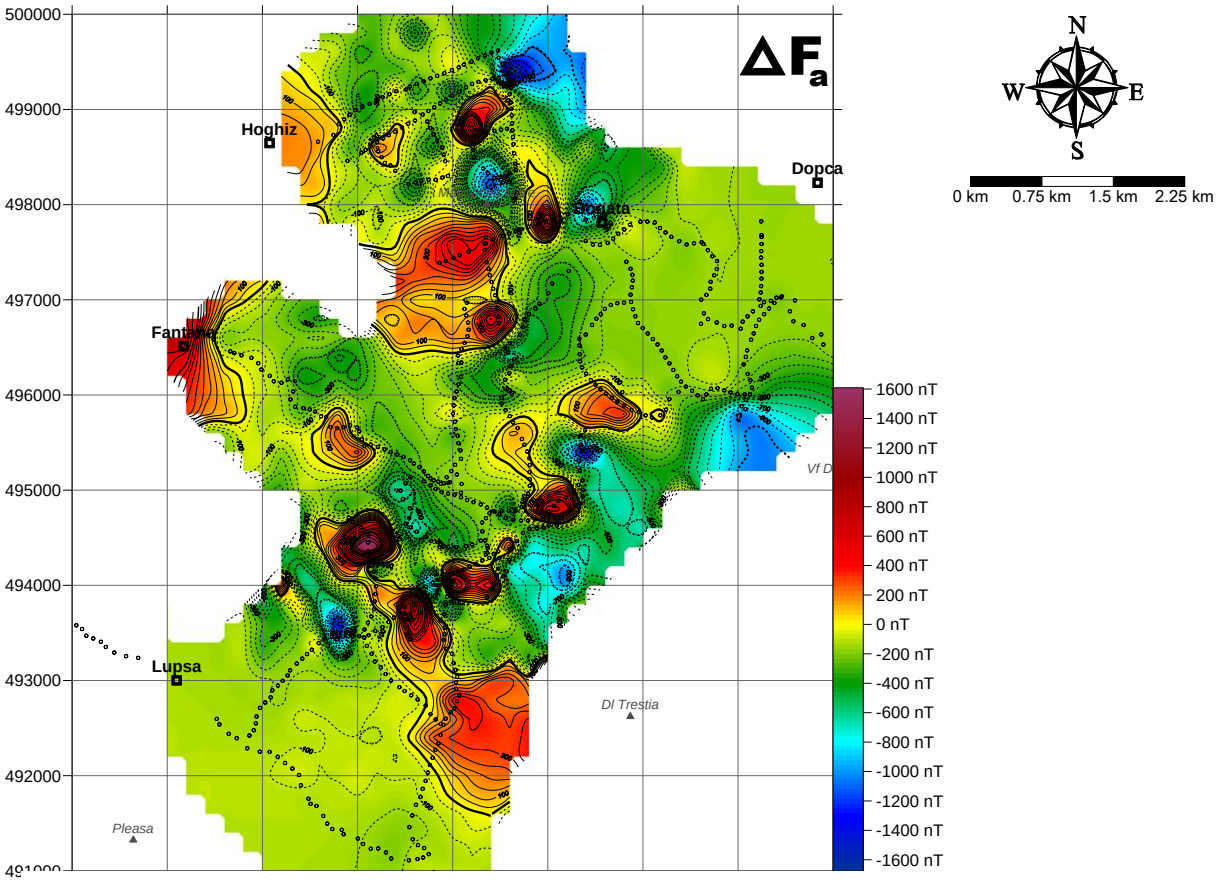

Fig. 38 - PERSANI AREA: Ground total intensity scalar geomagnetic anomaly

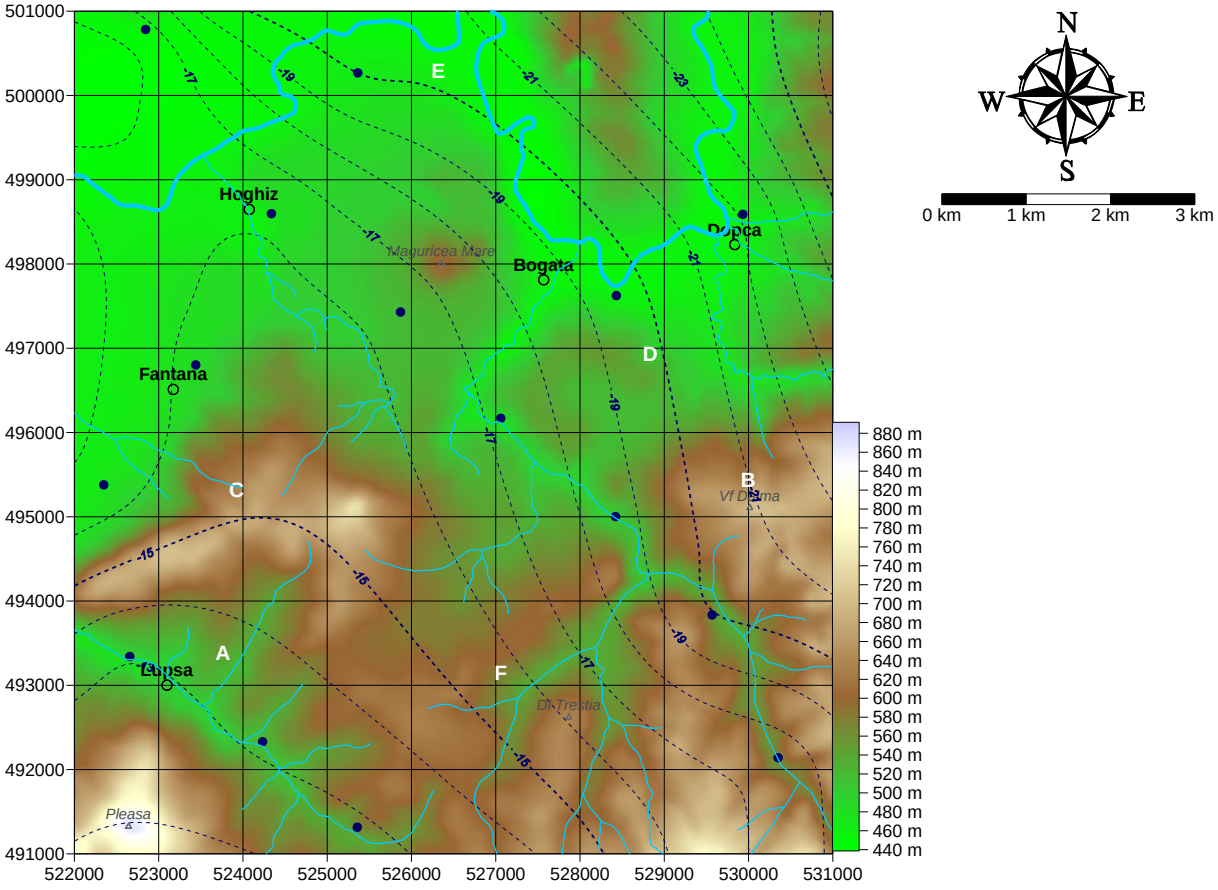

Fig. 39 - PERSANI AREA: Bouguer anomaly for 2.67 g/ccm reference density versus topography

ROCK SAMPLING AND PRESERVING

During the geophysical surveys within the Persani area, additional activities for sampling outcrops were conducted.

In the next figure, blue stars mark location of the sampled outcrops.

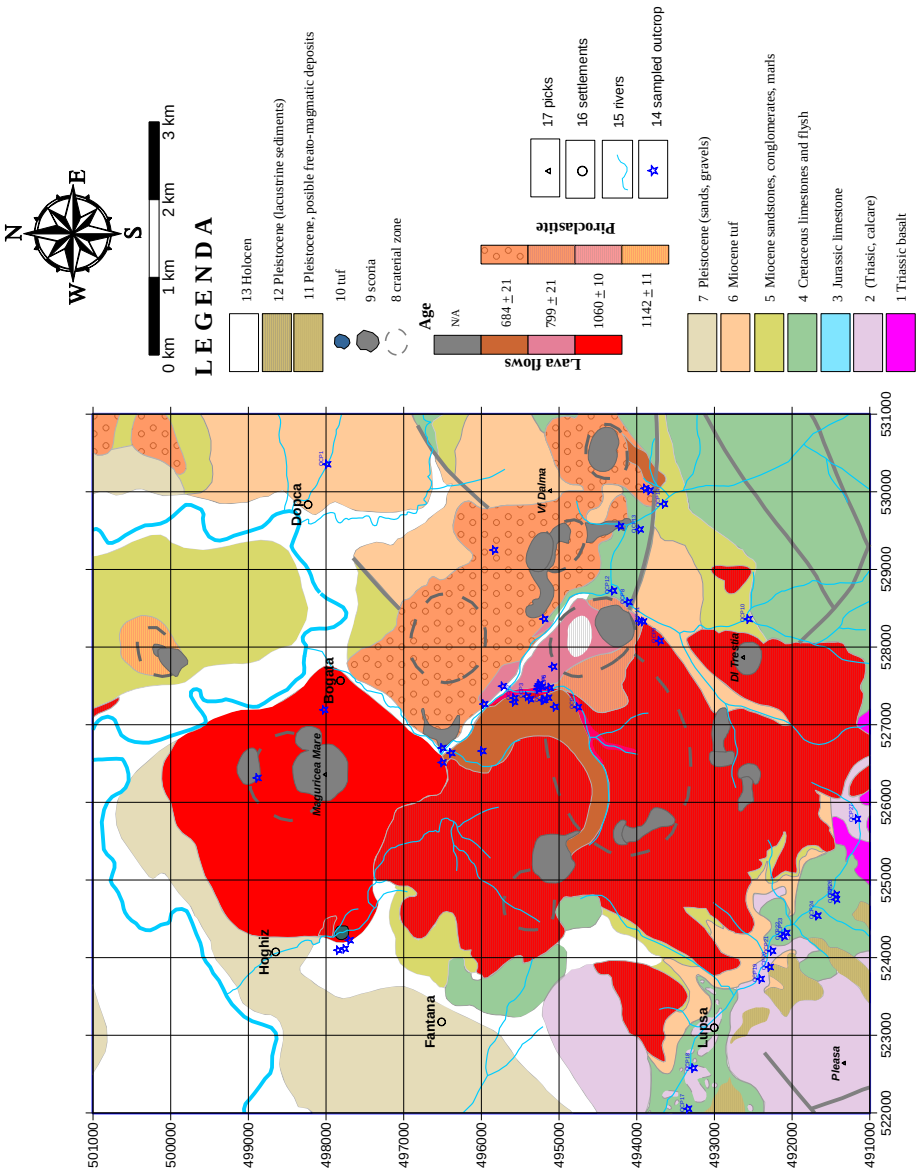

Fig. 40 - PERSANI AREA: Location of the sampled outcrops for rock-physics determination

Samples collected by the geophysical team are stored in the especially designed DDGT warehouse, and prepared for specific weight and magnetic susceptibility determinations.

Fig. 41 - DDGT ESPECIALLY DESIGNED DEPOSIT FOR PRESERVING ROCK SAMPLES AIMED AT ROCK PHYSICS DETERMINATIONS

SPECIFIC WEIGHT DETERMINATIONS

Specific weight determinations were conducted in the DDGT rock-physics lab by the double-weighting (air/water) methodology using a high accuracy analytical ballance.

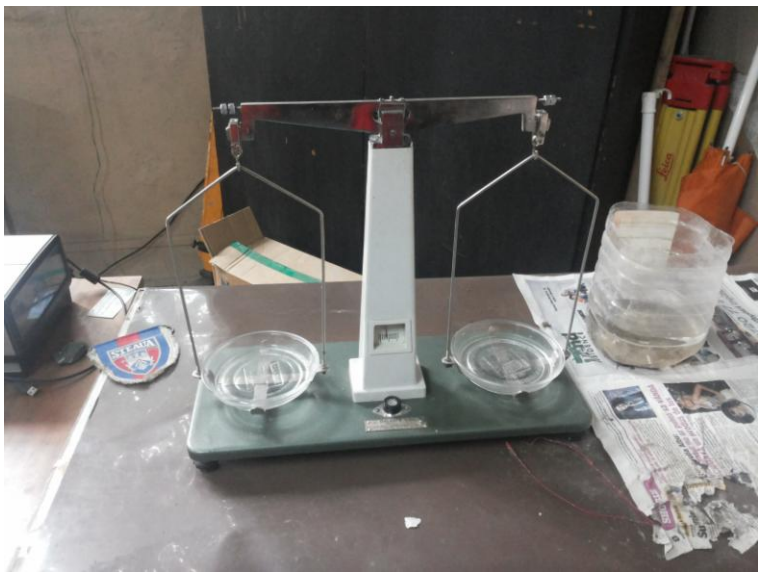

Fig. 42 - ANALYTICAL BALLANCE FOR SPECIFIC WIGHT DETERMINATIONS

DETERMINATION OF ROCK MAGNETIC PROPERTIES

Rock sampling for paleomagnetic observations

About 50 special rock samples from Neogene volcanic rocks were employed for paleomagnetic determinations.

The study area corresponds to Persani Mts. (Racos quarry, Racos – Heghes, Comana, Valea Stanciului, Valea Saratii, Magiricea, Hoghiz, Valea Barc, Valea Bogata, Gruiu - Valea Stanii, Valea Pietrele).

Rock samples core of 2.5 cm diameter have been extracted by the help of a portable drilling device. The orientation of the core samples has been determined by employing a Brunton compass and a solar compass (see the next figure) where possible.

Fig. 43 - ROCK-SAMPLING FOR PALEOMAGNETIC DETERMINATIONS

Localisation of outcrops – Latitude (°), longitude (°) and altitude (m). Location of the sampled outcrops has been determined with a portable GPS Magellan Explorist 600.

Fig. 44 - GPS -Magellan Explorist 600

Paleomagnetic determinations were conducted in the Paleomagnetism Laboratory of the Bucharest University by the courtesy of Professor Cristian Panaiotu.

The lab has state-of-the-art facilities for the determinations of rock magnetic properties.

Determination of the magnetic susceptibility (K)

The observations on the magnetic susceptibility of the rock samples were performed by employing the MFK1A (AGICO) device (see the next figure)

Fig 45 - MFK1A (AGICO)

Determination of the natural remnant magnetisation (NRM)

NRM determinations have been conducted by the help of the spin magnetometer JR-6A (AGICO) credited with an accuracy of $2x10^{-6}$ A/m

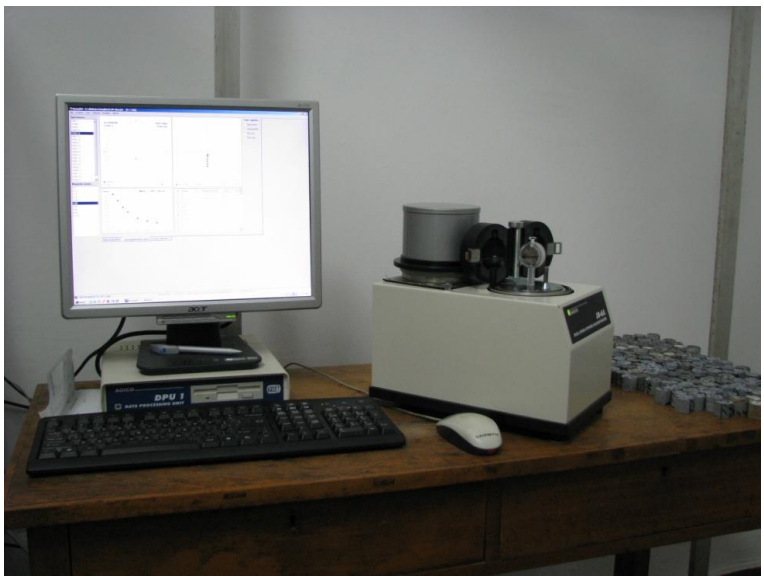

Fig. 46 - SPIN MAGNETOMETER JR-6A

(2) 3.3. ADVANCED DATA PROCESSING AIMED AT PROVIDING MORE INTUITIVE IMAGES FOR HELPING GEOLOGICAL INTERPRETATION

(2) 3.3.1. GENERAL CONSIDERATIONS

Unlike primary data processing aimed at providing consistency to various raw in order to offer coherent images of the investigated potential fields, the advanced data processing is intended to present some more intuitive images to researchers than the raw gravity/geomagnetic maps directly offered to interpreters by the raw observations.

The filtering approaches employed at this stage were as follows:

vertical gradient operator: aimed at emphasizing the shallow location of sources and more accurate outline of their contour; when comparing data offered by the potential fileds, the geomagnetic anomaly should be compared with the vertical gradient of the gravity (and not directly with the Bouguer anomaly) because it is the first derivative of gravity that has the same degree of spatial variability with the geomagnetic anomaly;

horizontal gradient operator: allows for an easier discrimination of cumulated effects belonging to various sources located at similar depths, and a better outline of the horizontal contour of the targets; it better reveals the presence of tectonic discontinuities (e.g. faults), but also inhomogeneities within datasets employed for the construction of the composite maps;

residual anomaly: may play a major role in the discrimination of the sources of different scale for the both geomagnetic and/or gravity anomalies;

reduced-to-the-pole geomagnetic anomaly: helps in the improved localising of the underground sources of the geomagnetic field: the vector-like features of magnetic properties may determine a lateral localisation of the anomaly apex as referred to the real position of the geomagnetic source: the reduce-to-pole approach acts like in the case of vertical magnetisation by bringing the geomagnetic effect above its source;

pseudo-gravity operator: computes the equivalent gravity effect of a contrast in magnetic properties based on Poisson relationship: this way it facilitates the interpretation because gravity effects are the result some density contrasts, which have a scalar nature, simpler than the vector nature of geomagnetic properties;

analytical signal operator: represents a mathematical approach that computes a synthetic anomaly, without a direct physical-geological equivalent, but which allows for an easier and more accurate outlining of the track of tectonic lineaments by avoiding distortions introduced by vector features of magnetic properties of the crust;

The above mentioned filters have been applied to currently obtained datasets of gravity and geomagnetic data, offering new images on the observed potential fields at the both regional (e,g, for INSTEC-SUD area), and local scale (e.g. CIOMADUL and PERSANI sub-perimeters).

Some examples are illustrated in the followings.

2.3.3.2. VERTICAL GRADIENT MAPS

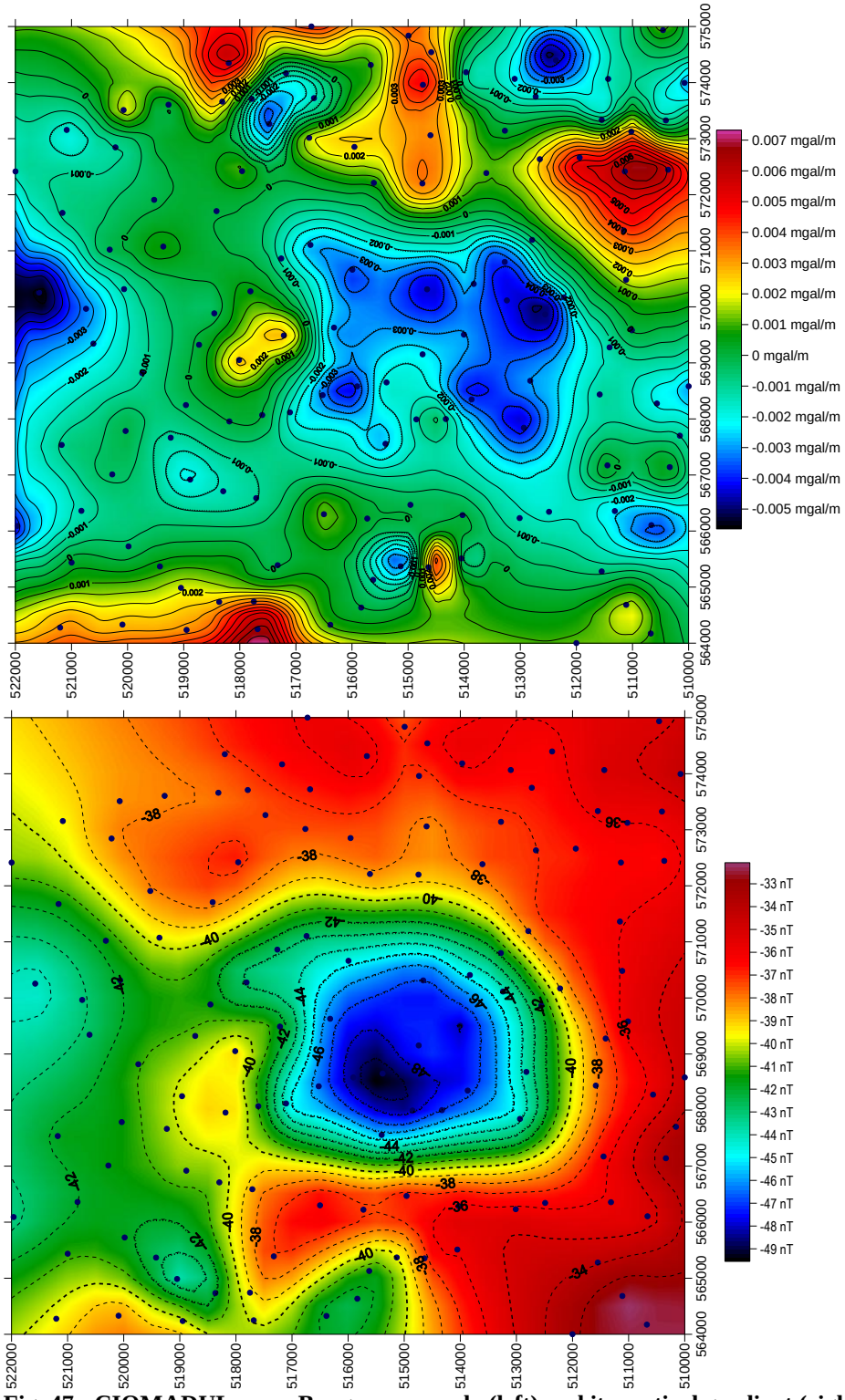

Fig. 47 - CIOMADUL area: Bouguer anomaly (left) and its vertical gradient (right)

(2) 3.3.3. HORIZONTAL GRADIENT MAPS

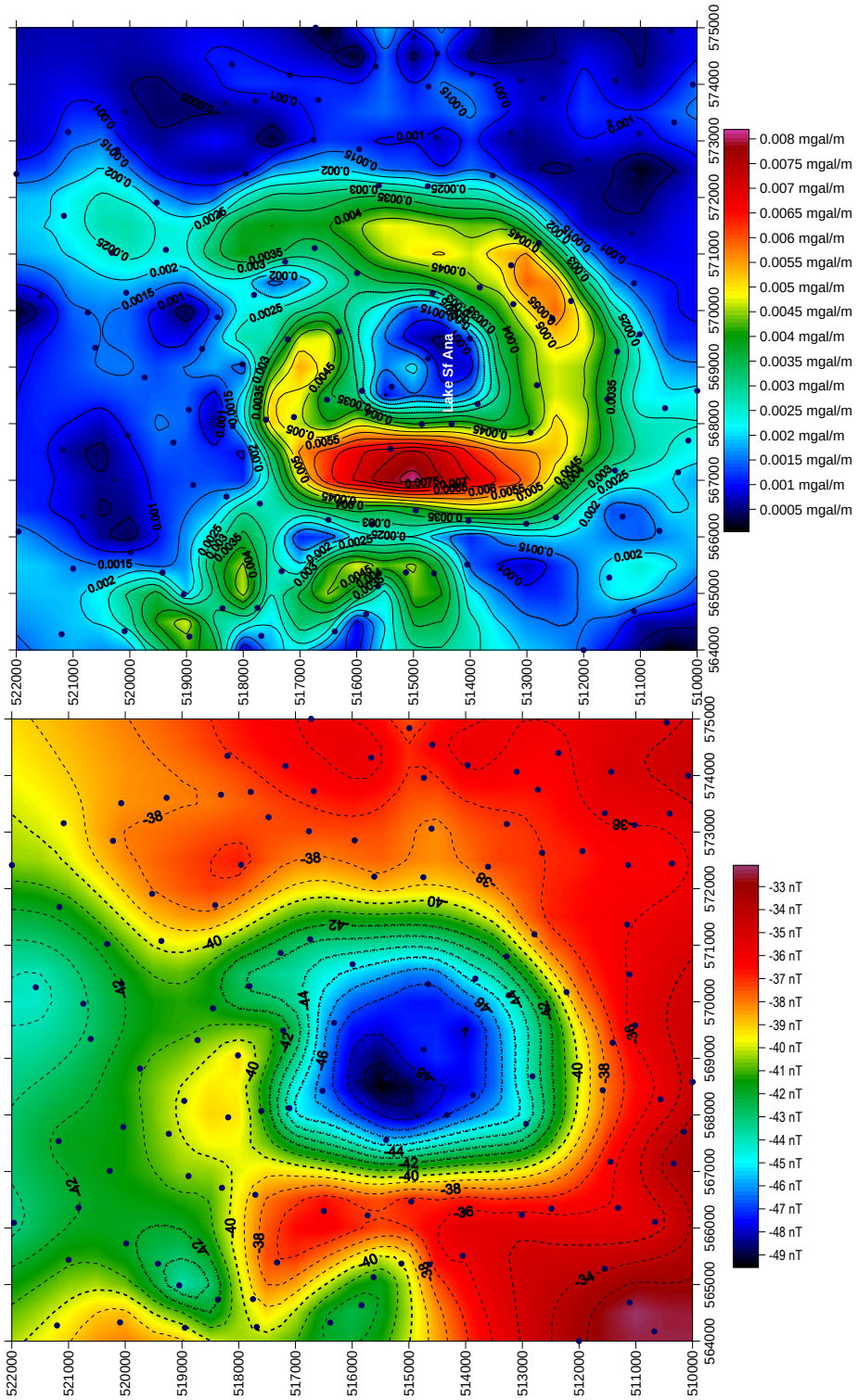

Fig. 48 - CIOMADUL area: Bouguer anomaly (left) and its horizontal gradient (right)

(2) 3.3.4. RESIDUAL ANOMALY MAPS

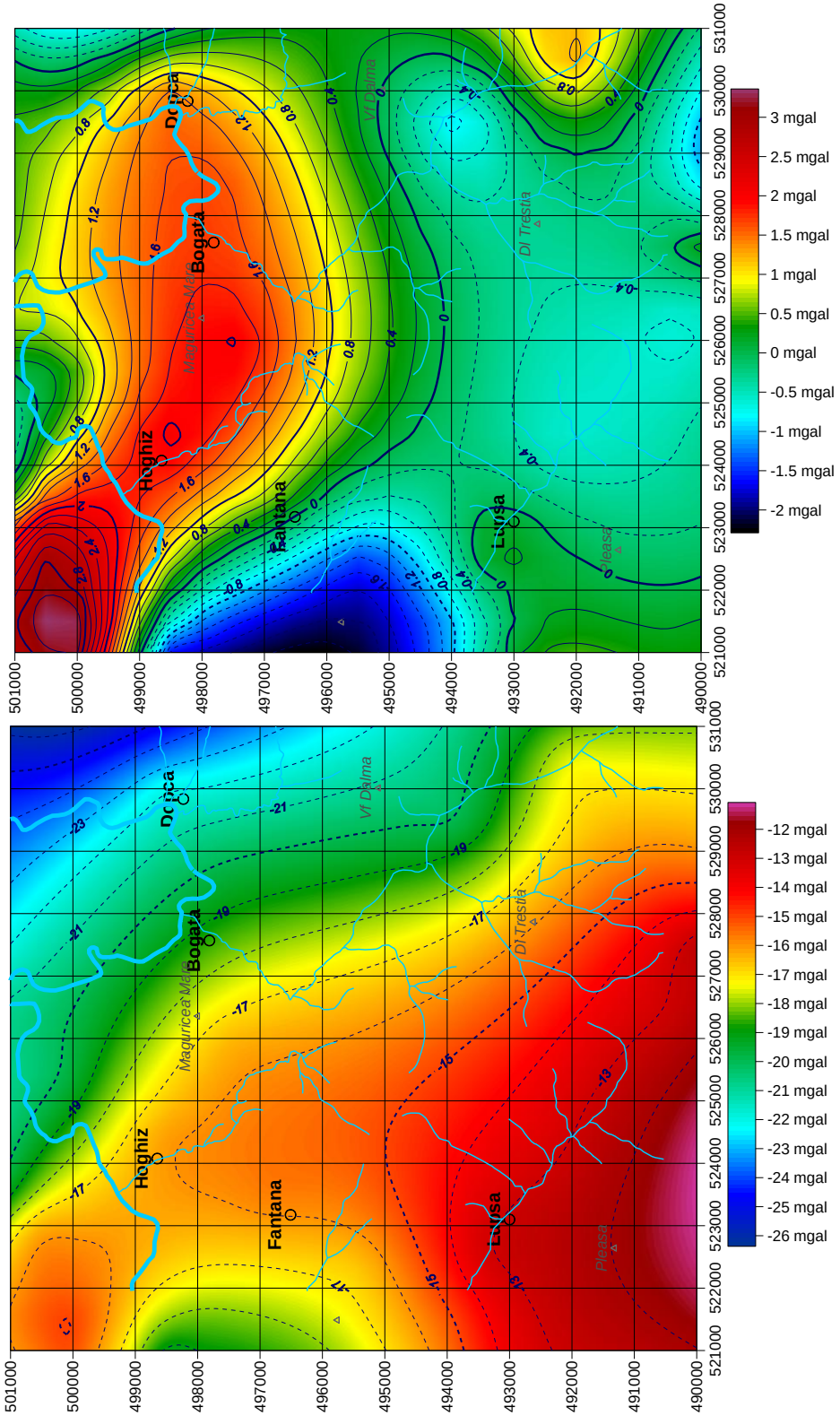

Fig. 49 - PERSANI area: Bouguer anomaly (left) and the residual anomaly as determined by subtratcing a third order polynomial trend (right)

(2) 3.3.5. GEOMAGNETIC ANOMALY REDUCED-TO-THE-POLE

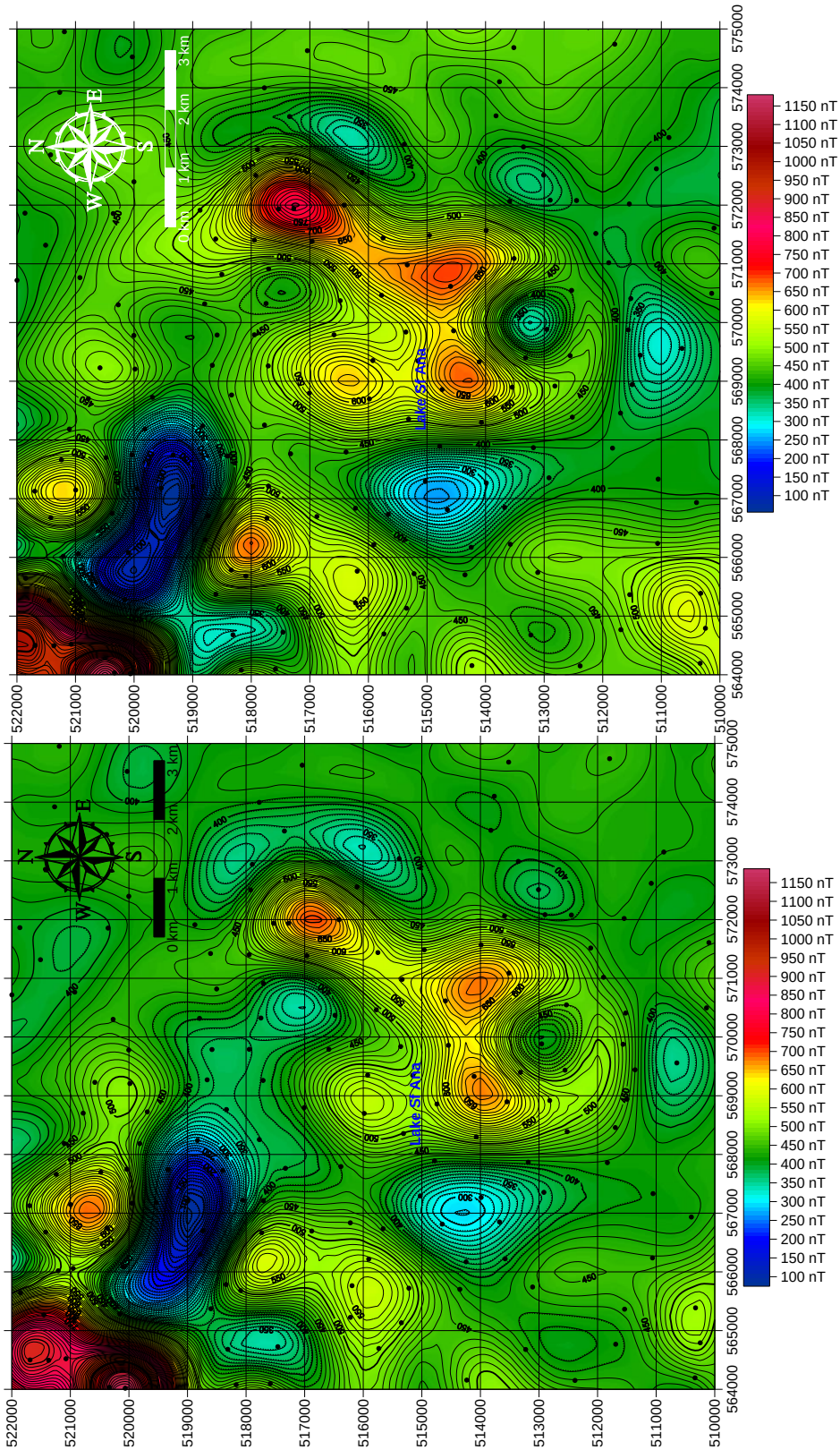

Fig. 50 - CIOMADUL area: Total intensity scalar geomagnetic anomaly (left) and the geomagnetic anomaly rediced-to-the-pole (right)

(2) 3.3.6. PSEUDO-GRAVITY MAPS

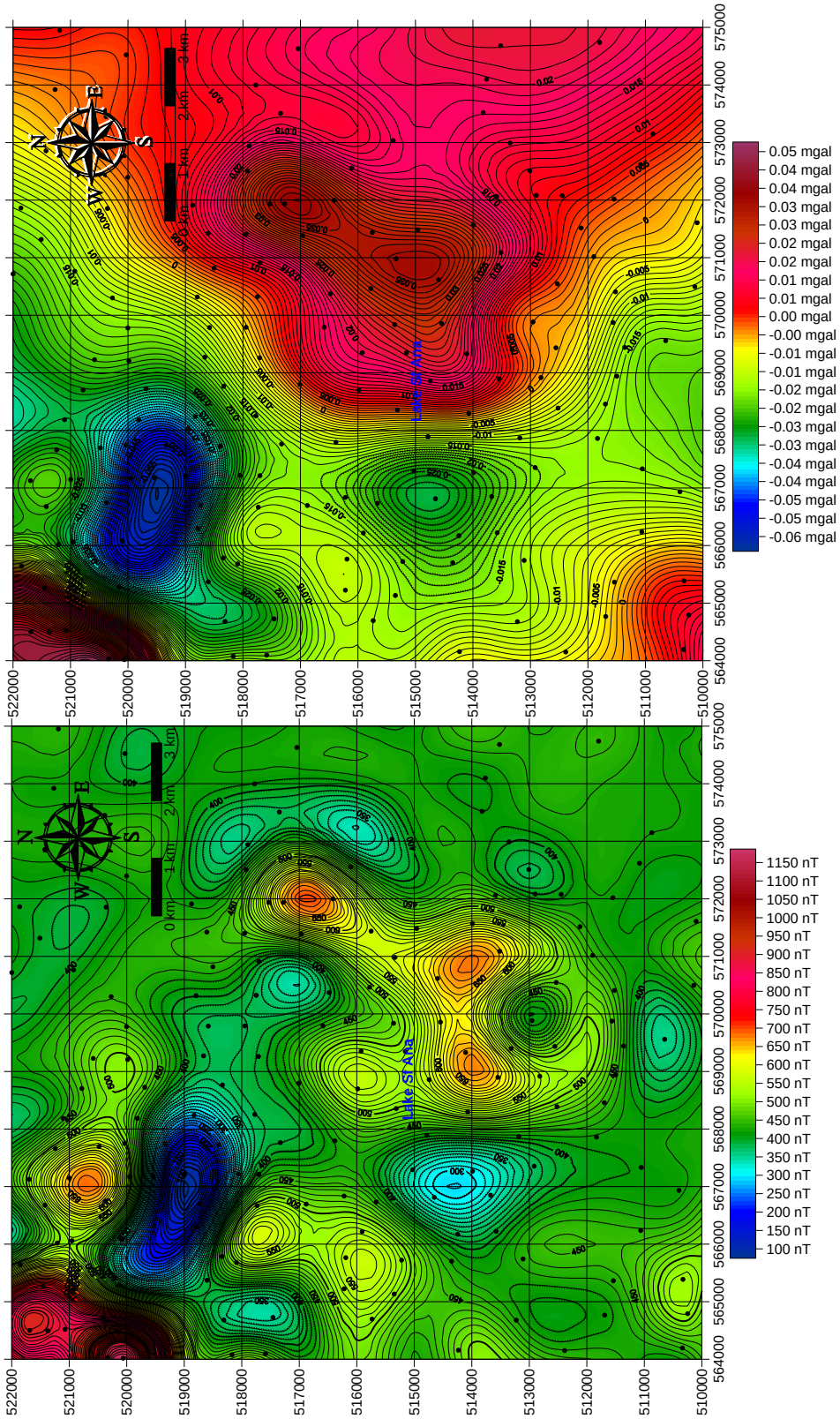

Fig. 51 - CIOMADUL area: Total intensity scalar geomagnetic anomaly (left) and the computed pseudo-gravity anomaly based on the Poisson relation (right)

(2) 3.3.7. ANALYTICAL SIGNAL MAPS

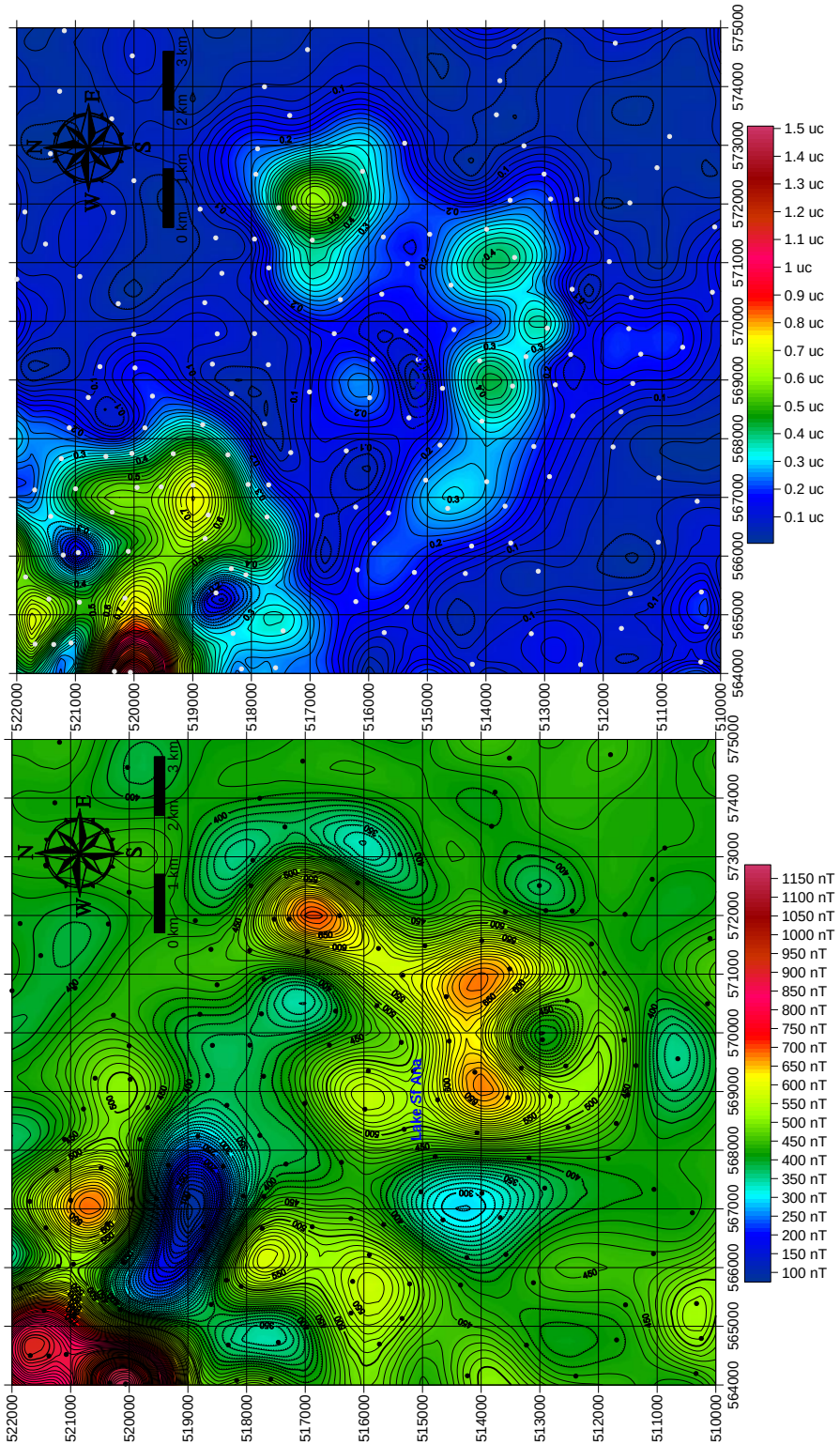

Fig. 52 - CIOMADUL area: Total intensity scalar geomagnetic anomaly (left) and the derived analytical signal (right)

D. DISEMINATION

(2) 4. DISEMINATION ACTIVITIES. ATTENDING THE NATIONAL AND INTERNATIONAL CONFERENCES ON THE PROPOSED THEMATIC

During 2014 we have participated to the following meetings:

EGU Viena between 27 April-2 May with presentation on proposed thematic and helping the preparation of the project, in the frame of international collaboration:

„Early Miocene Kırka-Phrigian caldera, western Anatolia - an example of large volume silicic magma generation in extensional setting" by **Ioan Seghedi** and Cahit Helvacı. Geophysical Research Abstracts Vol. 16, EGU2014-5789, EGU General Assembly 2014

and „Plagioclase and hornblende response to temperature and pressure induced variations in open magmatic systems. The example of Caraci Volcano, Apuseni Mts., by **Razvan-Gabriel Popa, Ioan Seghedi,** Theodoros Ntaflos, and Zoltan Pécskay. Geophysical Research Abstracts
Vol. 16, EGU2014-PREVIEW, EGU General Assembly 2014.

We have attended the International Congress **Carpatho-Balkanic Association, CBGA, Tirana, 2014** already with presentation related to our project data:

"Investigation of explosive volcanic structures by combined geological and geophysical surveys of Na-alkalic basaltic field in the Perşani Mts., Romania" by **Seghedi I., Beşutiu L., Popa R.-G., Szakács A., Atanasiu L., Vişan M**." in Proceedings of XX Congress of the Carpathian Balkan Geological Association Tirana, Albania, 24-26 September 2014, Special Issue vol.1, p 248.

"Time-space evolution and volcanological features of the Late Miocene-Quaternary Călimani-Gurghiu-Harghita volcanic range, East Carpathians, Romania. A review." By **Alexandru Szakács, Ioan Seghedi,** Zoltán Pécskay, **Viorel Mirea, Răzvan-Gabriel Popa**. in Proceedings of XX Congress of the Carpathian Balkan Geological Association Tirana, Albania, 24-26 September 2014, Special Issue vol.1, p. 249.

"Seismic and thermal properties of the upper mantle in the SE-Carpathian-Pannonian Region (CPR)" by Brandmayr E., **Seghedi I.,** Tumanian M., Panza G.F., in Proceedings of XX Congress of the Carpathian Balkan Geological Association Tirana, Albania, 24-26 September 2014, Special Issue vol.1, p. 427.

"Paleomagnetic constraints for the timing of volcanism from the Gurghiu, Harghita and Perşani Mountains (East Carpathians)", Panaiotu C., **Vişan, M. and Seghedi I**., in Proceedings of XX Congress of the Carpathian Balkan Geological Association Tirana, Albania, 24-26 September 2014, Special Issue vol.1, p. 247.

The preliminary petrological data on the Rodna-Bargau subvolcanic magmatic rocks has been presented in a **meeting of the Geological Society of Italy**:

"Petrological characterization of the upper Miocene Rodna-Bârgău sub-volcanic district (Eastern Carpathians, Romania)" by Laiena F., Fedele L., **Seghedi I.** & Morra V., 2014. Rend. Online Soc. Geol. It., Suppl. n. 1 al Vol. 31.

Selected references

Airinei, St., Stoenescu, Sc., Velcescu, G., Romanescu, D., Visarion, M., Radan, S., Roth, M., Besutiu, L. and Besutiu, G., 1983- La carte de l´anomalie magnétique ΔZ pour le territoire de la Roumanie. Anuarul Institutului de Geologie si Geofizica, seria Geofizica, Hidrogeologie si Geologie Inginereasca, **LXIII**, 5-11

Airinei, St., Stoenescu, Sc., Velcescu, G., Romanescu, D., Visarion, M., Radan, S., Roth, M., Besutiu, L. and Besutiu, G., 1985 - The geomagnetic anomaly ΔZ_a over the Romanian territory. Studii si cercetari geologice, geofizice si geografice, GEOFIZICA, **23**, 12-19 (in Romanian).

Atanasiu, L., Rosca V., Rogobete, M., 1996-A three-dimensional modelling of the East Carpathian Bend: 1st Congress of Balkan Geophysical Society, Abstr. Book, Athens, 266-267.

Besutiu L., Zlagnean L., Atanasiu L., 2012- The geomagnetic mapping of the Romanian Territory in the context of WDMAM Project, 7th EURGEO, Bologna, Italy,12-15 June 2012

Demetrescu, C., Nielsen, S.B., Ene, M., Şerban, D.Z., Polonic, G., Andreescu, M., Pop, A., Balling N., 2001-Lithosphere thermal structure and evolution of the Transylvanian Depression—insights from new geothermal measurements and modelling results, Physics of the Earth and Planetary Interiors, 126, 249–267

Demetrescu,C., Wilhelm, H., Ene, M., Andreescu, M., Polonic, G., Baumann, C., Dobrică, V., Şerban, D.Z.,2005- On the geothermal regime of the foreland of the Eastern Carpathians bend, Journal of Geodynamics 39 , p. 29-59

Hackney, R.I., Martin, M., Ismail-Zadeh, A.T., Sperner, B., Ioane, D., 2002- The gravity effect of the subducted slab beneath the Vrancea region, Romania, In: Michalik, J., Simon, L., Vozar, J. (Eds.), XVII Congress of the Carpathian-Balkan Geological Association, Geologica Carpathica, Bratislava, 119-121.

Hansen,R.O. şi Pawlowsky, R.S.,1989 – Reduction to the pole at low latitudes by Wiener filtering, Geophysics, 54, 1604-1613

Ioane, D., Radu, I., 1995- Global geopotential models and gravity data for the territory ofRomania, In: Sunkel, H., Marson, I. (Eds.), Gravity and Geoid. Joint IGC/ICG Symposium Graz, 1994, IAG Symposium No. 113, Springer, Heidelberg, 640-646.

Ioane, D., Atanasiu, L., 1998 - Gravimetric geoids and geophysical significances in Romania, In: Ioane, D. (Ed.) Monograph of Southern Carpathians, Rep. Geod., **7**(37), 157-175.

Ioane, D., Calota, C., Ion, D., 2005 - Deep geological structures as revealed by 3D gravity stripping: western part of the Moesian Platform, Romania. Journal of the Balkan Geophysical Society, Vol. 8, No. 3.

Ioane D., Ion D. , 2005 - A 3D crustal gravity modelling of the Romanian territory: JOURNAL OF BALKAN GEOPHYSICAL SOCIETY, Vol.8, No 4, November 2005, p.189-198

Korhonen, J. V., Fairhead J.D., Hamoudi M., Hemant K., Lesur V., Mandea M., Maus S., Purucker M., Ravat D., Sazonova T., and Thébault, E., 2007-Magnetic Anomaly Map of the World. *Map published by Commission for Geological Map of the World, supported by UNESCO, 1st Edition, GTK, Helsinki*. ISBN 978-952-217-000-2.

Mocanu, J.V şi Radulescu F.,1994 – Geophysical features of the Romanian territory, in.T.Berza, ed. ALCAPA II Field Guidebook: Geological Institute of Romania,p.17-36

Müller, B., 1993- Tectonic Stress in Europe. Borehole Guided Waves Affected by Stress – Induced Anysotropy. PhD.Thesis, University of Karlsruhe

Negoiţă, V., Zugrăvescu, D., Polonic, G., 2007- Upper crust regime of stresses according to the borehole measurements coming from Transylvanian Basin, Rev. Roum.Géophysique, 51, p. 3-14.

Seghedi, I., Szakács, Udrescu, Stoian, A.C. and Grabari, M. G., 1987- Trace elements geochemistry of the South Harghita volcanics (East Carpathians): calc- alkaline and shoshonitic associations, D.S. Inst. Geol. Geofiz. , vol. 72 - 73/1, 381 - 397.

Stănică, D., Stănică, M., Visarion, M., 1986 – The structure of the crust and upper mantle in Romania as deduced from magnetotelluric data, Revue.Roum. Geol.Geophys., Geophys., tom 30.

Panaiotu, C.G., Visan, M., Tugui, A., Seghedi, I., Panaiotu, A. G., 2012 - Palaeomagnetism of the South Harghita volcanic rocks of the East Carpathians: implications for tectonic rotations and palaeosecular variation in the past 5Ma, Geophys. J. Int, doi: 10.1111/j.1365-246X.2012.05394.

Veliciu, S., Šafanda, J., 1998- Ground temperature history in Romanian inferred from borehole temperature data, Tectonophysics, 291, 277-286

Visan, M., Panaiotu, C.G., Seghedi, I., 2014-Paleomagnetic constraints for the timing of volcanism from the South Gurghiu and Harghita Mountains, Revue Roumaine de Geophysique Tome 56–57.

Zugrăvescu , D., Polonic,G., Negoiţă,V., 2005 -Present state of stress determination in the Transylvanian basin using borehole measurements, St. cerc. Geofizică, tomul 43, p 3-14.

Zugrăvescu , D. şi Negoiţă,V., 2010 - Earth Upper Crust Regime of Stresses Inferred from Borehole Measurements on the Romanian Territory, Rev. Roum.Géophysique, 54, p. 55-64